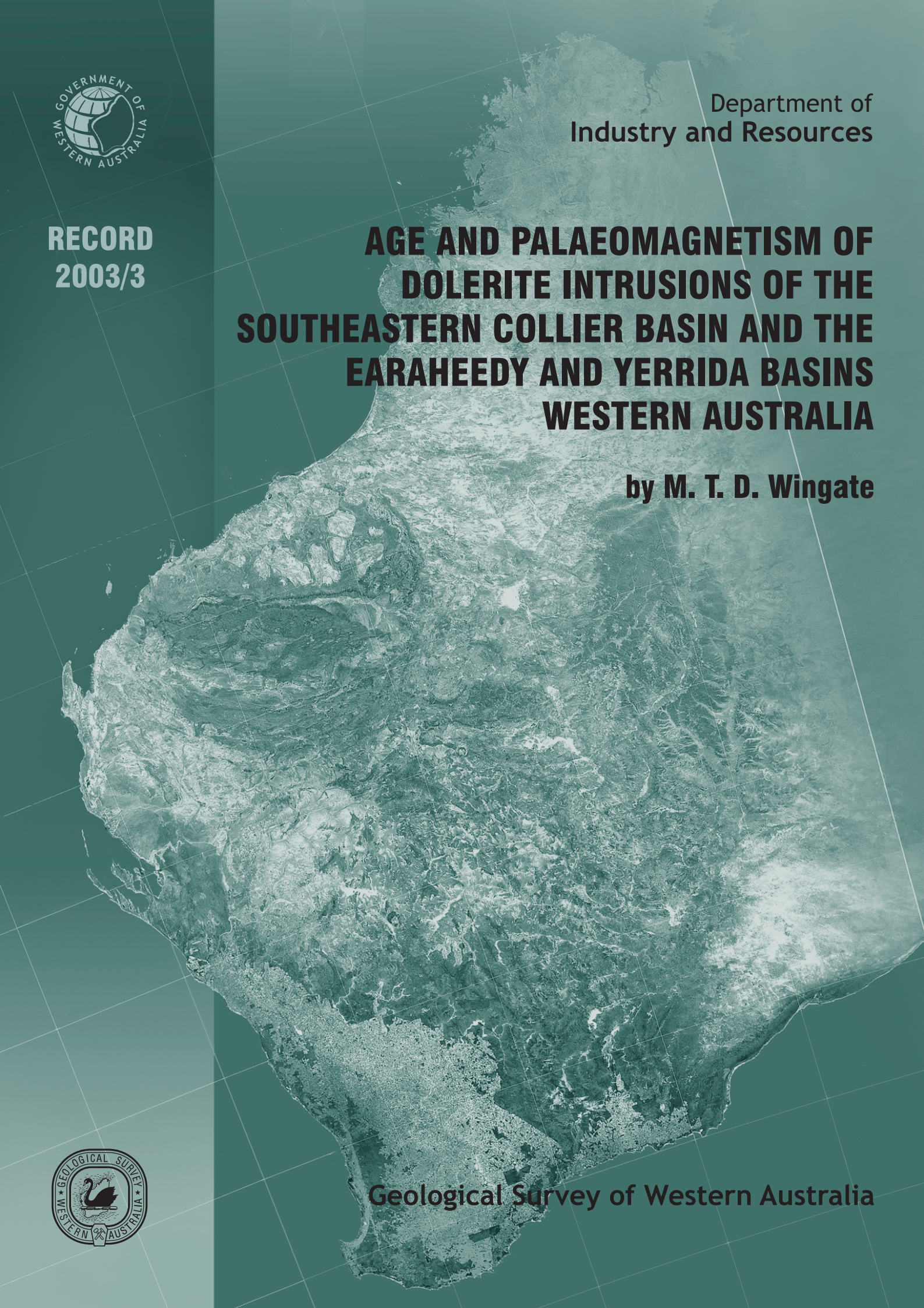

Department of
Industry and Resources

RECORD
2003/3

AGE AND PALAEOMAGNETISM OF DOLERITE INTRUSIONS OF THE SOUTHEASTERN COLLIER BASIN AND THE EARAHEEDY AND YERRIDA BASINS WESTERN AUSTRALIA

by M. T. D. Wingate

Geological Survey of Western Australia

GEOLOGICAL SURVEY OF WESTERN AUSTRALIA

RECORD 2003/3

AGE AND PALAEOMAGNETISM OF DOLERITE INTRUSIONS OF THE SOUTHEASTERN COLLIER BASIN, AND THE EARAHEEDY AND YERRIDA BASINS, WESTERN AUSTRALIA

by
M. T. D. Wingate

Tectonics Special Research Centre, School of Earth and Geographical Sciences,
The University of Western Australia, 35 Stirling Highway, Crawley, WA 6009

Perth 2003

MINISTER FOR STATE DEVELOPMENT
Hon. Clive Brown MLA

DIRECTOR GENERAL
DEPARTMENT OF INDUSTRY AND RESOURCES
Jim Limerick

DIRECTOR, GEOLOGICAL SURVEY OF WESTERN AUSTRALIA
Tim Griffin

REFERENCE
The recommended reference for this publication is:
WINGATE, M. T. D., 2003, Age and palaeomagnetism of dolerite intrusions of the southeastern Collier Basin, and the Earaheedy and Yerrida Basins, Western Australia: Western Australia Geological Survey, Record 2003/3, 35p.

National Library of Australia Card Number and ISBN 0 7307 8906 3

Grid references in this publication refer to the Geocentric Datum of Australia 1994 (GDA94). Locations mentioned in the text are referenced using Map Grid Australia (MGA) coordinates, Zone 51. All locations are quoted to at least the nearest 100 m.

Printed by The Digital Document Company Pty Ltd, Perth, Western Australia

Published 2003 by Geological Survey of Western Australia

Copies available from:
Information Centre
Department of Industry and Resources
100 Plain Street
EAST PERTH, WESTERN AUSTRALIA 6004
Telephone: (08) 9222 3459 Facsimile: (08) 9222 3444
This and other publications of the Geological Survey of Western Australia are available online through the Department's bookshop at www.doir.wa.gov.au

Contents

Appendices

Figures

Tables

Age and palaeomagnetism of dolerite intrusions of the southeastern Collier Basin, and the Earaheedy and Yerrida Basins, Western Australia

by

M. T. D. Wingate[1]

Abstract

Integrated U–Pb geochronology and palaeomagnetism of the Glenayle Dolerite have been used to determine whether siliciclastic sedimentary rocks of the Salvation Group, on the STANLEY 1:250 000 map sheet, correlate with Mesoproterozoic rocks of the Edmund and Collier Basins or with Neoproterozoic rocks of the northwestern Officer Basin.

Ion microprobe U–Pb baddeleyite geochronology of two dolerite samples yielded mean $^{207}Pb/^{206}Pb$ ages of 1068 ± 20 and 1063 ± 21 Ma. These data are combined to yield a mean age of 1066 ± 14 Ma, which is interpreted as the age of intrusion of the Glenayle Dolerite. This is a minimum age for deposition of the Salvation Group, and rules out any correlation with Neoproterozoic rocks of the Sunbeam Group.

Palaeomagnetic measurements were conducted on samples from ten sites in the Glenayle Dolerite, including the two dated sites, and from a single site in the Prenti Dolerite of the Palaeoproterozic Earaheedy Basin. All sites yield a stable magnetization component directed to the north-northwest with moderate downward inclination. Based on rock magnetic and palaeomagnetic evidence for the presence of single-domain magnetite, and on agreement with primary palaeomagnetic directions observed in dolerites of the same age in the western Edmund and Collier Basins, the Glenayle and Prenti magnetizations are inferred to be primary thermoremanent magnetizations acquired during sill emplacement and cooling at 1066 Ma. Combined data for the Glenayle and Prenti Dolerites yield a palaeomagnetic pole at 33°N, 109°E, and indicate a palaeolatitude of 30°30'N for the Salvation Group at 1066 Ma. The sampled dolerites probably represent an insufficient number of separate intrusions, however, to have adequately averaged palaeosecular variation of the Earth's magnetic field. Agreement of palaeomagnetic data from across the Edmund and Collier Basins implies that no significant vertical axis rotations have affected the Capricorn Orogen since 1070 Ma.

The similarity of isotopic ages and palaeomagnetic poles of the Glenayle and Prenti Dolerites, and dolerites from the western Edmund and Collier Basins indicate that these rocks were emplaced during the same magmatic event at c. 1070 Ma. Similar ages have been determined for mafic igneous rocks in the northwestern Yilgarn Craton, at the base of the Empress 1A drillhole in the western Officer Basin, and in the Musgrave Complex of central Australia, suggesting that these rocks belong to a single large igneous province (LIP). Widespread magmatism across western and central Australia at this time was synchronous with deformation and magmatism in the Pinjarra Orogen, late-stage deformation in the Albany–Fraser Orogen, and possibly with deformation of the western Edmund and Collier Basins during the Edmundian Orogeny.

Comparison of late Mesoproterozoic palaeomagnetic data for Australia and Laurentia does not support previous reconstructions of Australia–Antarctica against either western Canada (the SWEAT hypothesis) or the western United States (the AUSWUS hypothesis). The data permit a 1070 Ma reconstruction (AUSMEX: Australia–Mexico) that closely aligns late Mesoproterozoic orogenic belts in northeastern Australia and southernmost Laurentia. However, a preliminary assessment of c. 1.2 Ga palaeopoles does not support a late Mesoproterozoic connection between Australia and Laurentia, although a 25 million-year mismatch in age could mask significant latitudinal motion of either continent.

A reconnaissance palaeomagnetic and rock magnetic survey was conducted on samples from four sites in altered dolerite sills of the Killara Formation in the Palaeoproterozoic Yerrida Basin. The magnetizations of these rocks are of low stability, with unblocking temperatures below 350°C, and are directed inconsistently, both within and between sites. These magnetizations are interpreted as overprints resulting mainly from alteration, possibly during the 1.83 to 1.78 Ga Capricorn Orogeny, or from weathering. No coherent palaeomagnetic component could be determined for the Killara Formation sills.

KEYWORDS: Australia, Collier Basin, dolerite, sills, geochronology, Glenayle Dolerite, Mesoproterozoic, palaeomagnetism, Palaeoproterozoic, Salvation Group, Yerrida Basin.

[1] Tectonics Special Research Centre, School of Earth and Geographical Sciences, The University of Western Australia, 35 Stirling Highway, Crawley, WA 6009.

Introduction

Purpose and scope

This Record describes an investigation into the age and palaeomagnetic characteristics of a suite of dolerite sills, known as the Glenayle Dolerite (Hocking et al., 2000), that intrude sedimentary rocks of the Salvation Group in the southeastern Collier Basin in the area around Glenayle Homestead, mainly on the STANLEY* 1:250 000 map sheet (Commander et al., 1982; Fig. 1). Rocks of the Salvation Group were considered initially to be part of the Bangemall Supergroup, and therefore of Mesoproterozoic age (Muhling and Brakel, 1985). Bagas et al. (1999) and Hocking et al. (2000), however, correlated parts of the succession with the Neoproterozoic Sunbeam Group of the Officer Basin.

This study was initiated to distinguish between these alternatives by comparing palaeomagnetic characteristics of the Glenayle Dolerite with those of other studied Proterozoic rocks, in particular the 1070 Ma BBS pole from dolerite sills in the western Bangemall Supergroup (Wingate, 2002), and, if possible, by direct U–Pb dating of the Glenayle Dolerite using the sensitive high-resolution ion microprobe (SHRIMP). The project was extended to study a dolerite sill, referred to as the Prenti Dolerite, intruding Palaeoproterozoic rocks of the adjacent Earaheedy Basin, that may be equivalent in age to the Glenayle Dolerite. The implications of the geochronological and palaeomagnetic results for regional tectonics and continental reconstructions are discussed briefly. Also reported here are the results of a reconnaissance palaeomagnetic study of Palaeoproterozoic dolerite sills in the Yerrida Basin (Pirajno and Adamides, 2000).

Location and access

The Glenayle Dolerite was studied on the STANLEY and southwestern TRAINOR 1:250 000 map sheets (Fig. 1; Commander et al., 1982; Williams, 1995). Palaeomagnetic sampling concentrated on the MUDAN and GLENAYLE 1:100 000 sheets (on STANLEY), which have recently been remapped in detail (Pirajno and Hocking, 2001, 2002). A dolerite sill near Prenti Downs Homestead, south of Lake Carnegie, on the VON TREUER 1:100 000 map sheet (on KINGSTON 1:250 000), was also sampled.

Palaeoproterozoic dolerite sills of the Yerrida Basin were sampled at three localities north of Wiluna, on the CUNYU (on WILUNA 1:250 000) and THADUNA (on PEAK HILL 1:250 000) 1:100 000 map sheets, and at one locality farther west, northeast of Killara Homestead, on the GLENGARRY 1:100 000 map sheet (on GLENGARRY 1:250 000). All study areas are on land held as Pastoral Leases and year-round access is via graded shire roads and station tracks.

* Capitalized names refer to standard 1:100 000 and 1:250 000 map sheets.

Dolerite sills in the southeastern Collier Basin and Earaheedy Basin

Geological setting

The Edmund and Collier Basins, known previously as the 'Bangemall Basin' (Muhling and Brakel, 1985), are intracratonic basins of Mesoproterozoic age located between the Pilbara and Yilgarn Cratons (Fig. 1). Sedimentary successions within the Edmund and Collier Basins consist of the Edmund Group and the overlying Collier Group, which together comprise the Bangemall Supergroup (Martin et al., 1999; Martin and Thorne, 2002). The Edmund and Collier Groups unconformably overlie rocks that were deformed or metamorphosed (or both) during the 1.83 to 1.78 Ga Capricorn Orogeny, which resulted from the collision of the Pilbara and Yilgarn Cratons (Tyler and Thorne, 1990; Occhipinti et al., 1999).

The Collier Group contains up to 3 km of siltstone and sandstone (Martin et al., 1999), and incorporates the previous Karbhan, Manganese, Mucalana, and Collier Subgroups, and possibly the Oldham and Ward Inliers within the northwestern Officer Basin (Muhling and Brakel, 1985; Williams, 1990; Hocking et al., 2000). The Scorpion Group, which contains up to 10 km of carbonate and fine to coarse clastic rocks, unconformably underlies the Collier Group (Fig. 1) and has been correlated with the Edmund Group (Williams, 1990). The Bangemall Supergroup is overlain unconformably by Neoproterozoic strata of the Sunbeam Group, which is part of the northwestern Officer Basin (Bagas et al., 1999).

The Bangemall Supergroup contains large volumes of tholeiitic dolerite sills (Muhling and Brakel, 1985). Two suites of sills in the western part of the region gave SHRIMP U–Pb zircon and baddeleyite ages of 1465 ± 3 and 1070 ± 6 Ma (Wingate, 2002). The older sills are apparently restricted to the Edmund Group, whereas the younger suite is present in both the Edmund and Collier Groups. The Collier Group was therefore deposited before 1070 Ma. The Edmund Group is older than 1465 Ma (Wingate, 2002), and younger than 1619 ± 15 Ma monzogranite in the underlying Gascoyne Complex (Nelson, 1998; Sheppard and Swager, 1999). The tectonic controls on dolerite magmatism within the Bangemall Supergroup are not clear, although the 1070 Ma episode was synchronous with metamorphic and igneous activity in the Pinjarra Orogen (Harris, 1995; Bruguier et al., 1999), and with mafic magmatism in the Musgrave Complex of central Australia (Glikson et al., 1996; Zhao and McCulloch, 1993).

Resolving the ages, stratigraphic relationships, and correlation of sedimentary rocks in the southeastern part of the Collier Group has been problematic, however, and several revisions have been proposed in recent years. Defined originally as the Kahrban Subgroup of the Mesoproterozoic Bangemall Group by Muhling and Brakel (1985), parts of the succession (Jiliyili, Brassey Range, and Coonabildie Formations; Fig. 2) were correlated with the Neoproterozoic Sunbeam Group by Bagas et al. (1999) and

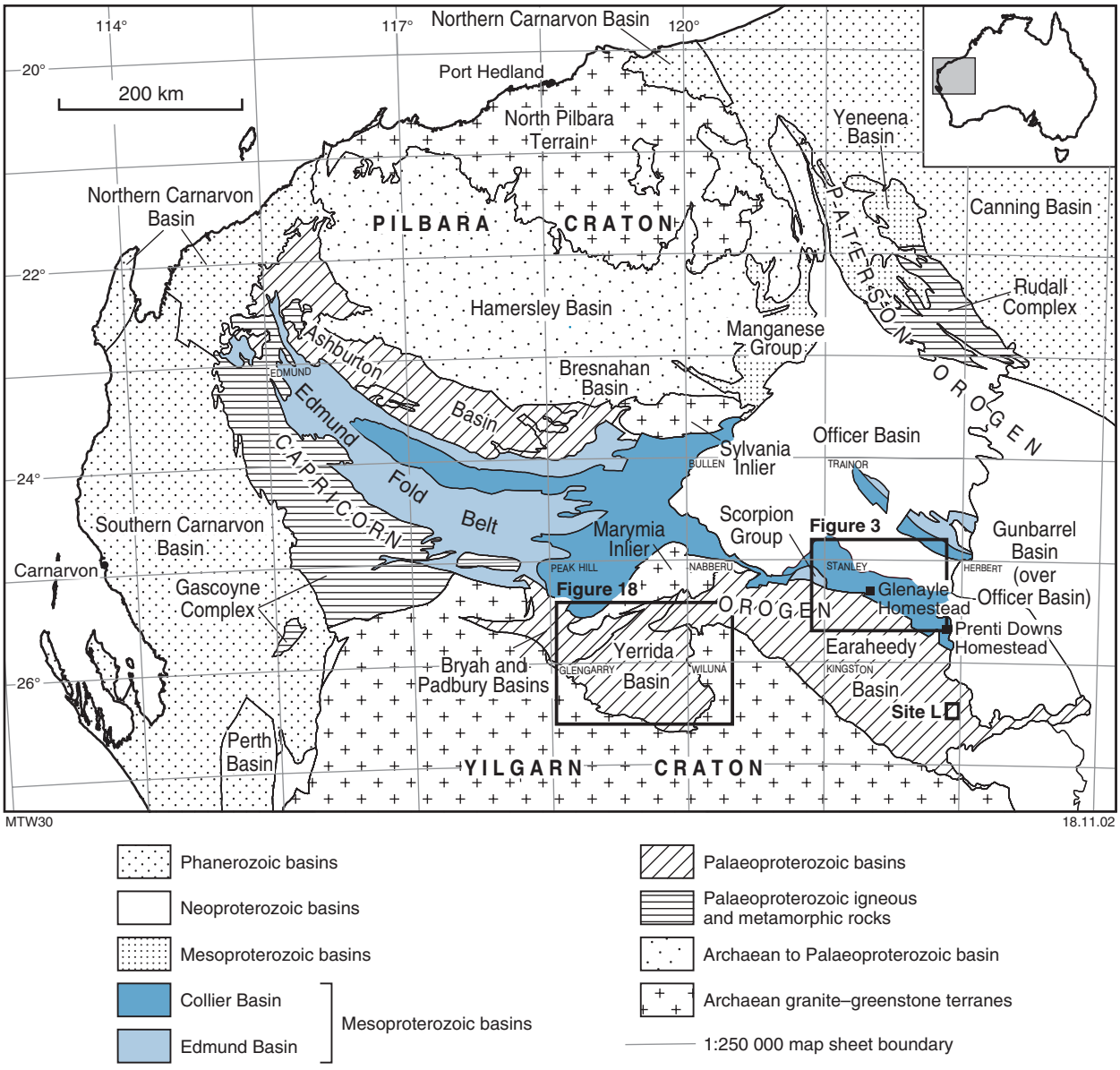

Figure 1. Regional geological setting of the Edmund, Collier, and Yerrida Basins. Boxes show the areas studied. The 1:250 000 map sheets on which work was carried out are named, including the EDMUND sheet worked on by Wingate (2002)

Hocking et al. (2000). However, preliminary palaeomagnetic directions for the Glenayle Dolerite, which intruded these formations, were recognized as similar to those obtained from 1070 Ma dolerite sills in the western part of the Bangemall Supergroup (Wingate, 2002). Based on these initial palaeomagnetic results, and also on stratigraphic and palaeocurrent information and subsequent K–Ar dating, the Jiliyili, Brassey Range, and Coonabildie Formations were recognized as older than the Officer Basin strata, but possibly younger than the Collier Group, and were assigned by Hocking and Jones (2002) to a new unit — the Salvation Group (Fig. 2).

Glenayle Dolerite sills and the enclosing Salvation Group sedimentary rocks are generally flat lying or very gently folded, with dips typically less than 5° (Commander et al., 1982; Pirajno and Hocking, 2001, 2002). Sills typically exceed 100 m in thickness, and chilled margins are exposed in places. The number of separate intrusions comprising the Glenayle Dolerite is unknown, and could be as low as one or two. The K–Ar ages of 917 ± 13 and 968 ± 19 Ma (both ±2σ) determined for K-feldspar from two samples of granophyric Glenayle Dolerite (Fig. 3) are interpreted as minimum estimates of the time of dolerite crystallization (Nelson, 2002). Compston (1974) and Preiss et al. (1975) reported Rb–Sr and K–Ar ages of c. 1050 Ma for dolerite sills intruding sedimentary rocks of the adjacent Earaheedy Basin on the ROBERT 1:250 000 map sheet.

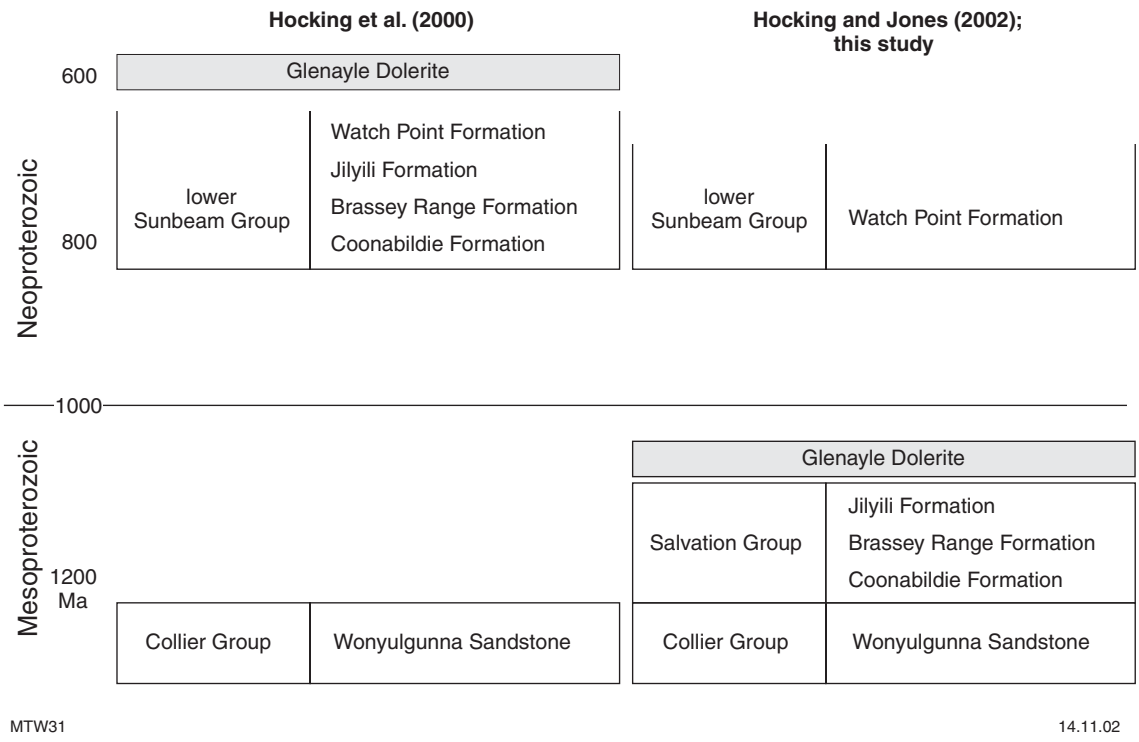

Figure 2. Stratigraphic correlation of the Salvation Group

Petrography of dolerite sills

The Glenayle Dolerite consists of fine- to medium-grained microgabbro sills and dykes. Three different types of dolerite were recognized by Pirajno and Hocking (2002), all containing variable amounts of granophyre:

- very fine to medium-grained basaltic rock with abundant (typically 5 to 7%) disseminated Fe–Ti oxides and minor sulfide grains;
- fine- to medium-grained dolerite containing distinct millimetre-scale blebs of pink quartz–K-feldspar granophyre, also commonly with abundant Fe–Ti oxides;
- medium- to coarse-grained gabbro, locally mesocratic and granophyric. Most samples contain plagioclase (labradorite $An_{60–72}$, ~50% by volume), augite (~35%), and more rarely pigeonite or enstatite, with textures ranging from typically ophitic to intergranular. Interstitial quartz–orthoclase (locally adularia) granophyre increases (up to 20–30%) towards the tops of sills. Accessory minerals include disseminated Fe–Ti oxides, quartz, apatite, biotite, hornblende, chlorite, and prehnite.

The Glenayle Dolerite is intruded by aphanitic to very fine grained dolerite sills and dykes, referred to as the Prenti Dolerite by Pirajno and Hocking (2002). This rock is petrographically similar to the sill intruding the Earaheedy Group (at site L, Fig. 1). The Prenti Dolerite typically contains plagioclase ($An_{56–70}$, 50–55%) and granular augite (partially replaced by chlorite and biotite), with an intergranular–glomeroporphyritic texture. In some samples disseminated Fe–Ti oxides comprise up to 10% of the rock. It has not been determined whether the Glenayle and Prenti Dolerites are comagmatic or represent separate magmatic events.

Geochronology

Samples for U–Pb geochronology were obtained from two sites (Appendix 1) in dolerite sills that were also sampled for palaeomagnetism (Fig. 3). All material was trimmed in the field to yield about 20 kg of unweathered rock. The most coarse grained differentiated rocks were selected as the most likely to contain zircon or baddeleyite. Zircon is relatively rare in mafic intrusions, and is of xenocrystic origin in many cases (e.g. Black et al., 1991). Baddeleyite (ZrO_2) is a trace constituent in many mafic intrusions, in which it typically forms small (<100 μm long), pleochroic brown crystals with monoclinic (2/m) symmetry and tabular habit. Baddeleyite has a high blocking temperature (similar to zircon), is enriched in uranium, has very low initial lead, is highly resistant to loss of radiogenic lead, and is highly unlikely to form xenocrysts in mafic intrusions (Heaman et al., 1992; Heaman and LeCheminant, 1993; Wingate, 2000). Baddeleyite is therefore ideal for accurately dating the crystallization of mafic intrusive rocks by the U–Pb method.

Sample preparation and analytical procedures

For each sample about 800 g of rock (crushed to <250 μm) was washed carefully to remove fines, then processed by

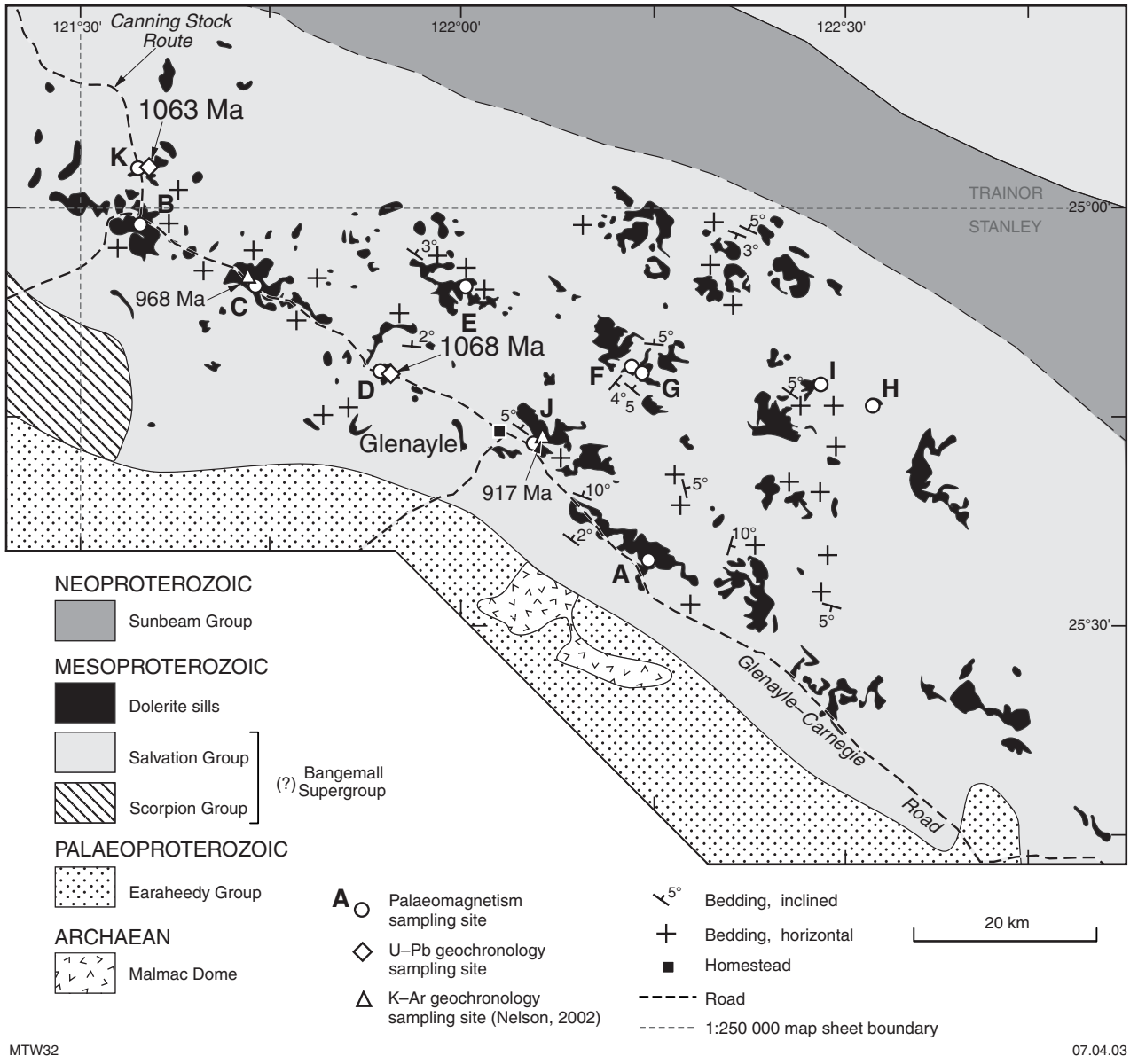

Figure 3. Simplified geological map of Glenayle Dolerite sills intruding the Salvation Group on the STANLEY and adjacent 1:250 000 map sheets. The locations of samples collected during this study for palaeomagnetism (circles) and U–Pb geochronology (diamonds) are indicated. The U–Pb ages are interpreted as accurate estimates of the time of dolerite crystallization. Also shown are locations of samples dated by K–Ar (triangles) at sites C and J; ages were interpreted as minimum estimates of the time of crystallization (Nelson, 2002)

conventional magnetic and density techniques to concentrate nonmagnetic heavy fractions. Although no zircons were recovered, the two samples each yielded between 50 and 70 baddeleyite crystals, which were hand-picked from concentrates under a binocular microscope.

All crystals are pleochroic, from light to dark brown, and most are either euhedral crystals or broken fragments of euhedral crystals. They reach up to 100 μm in length and 30 to 50 μm in width. Crystal surfaces are typically clean and smooth, with no evidence of secondary zircon overgrowths, which can form by interaction of baddeleyite with silica-bearing fluids during metamorphism or alteration (e.g. Wingate et al., 1998). Several crystals contain central cavities or channels (Fig. 4) — a textural feature indicative of rapid crystallization at shallow crustal levels (Lofgren, 1980; Brossart et al., 1986).

Crystals from the two samples, together with a baddeleyite reference standard, were cast in an epoxy mount, which was then polished to section the crystals for analysis. About 30% of the crystals were lost during polishing because of their very thin, tabular habit. The mount was cleaned thoroughly, and the polished surface was documented with transmitted and reflected light micrographs, then vacuum coated with an approximately 500 nm layer of high-purity gold. To eliminate any residual water from the sampling surface, the mount was pumped down to high vacuum overnight in the ion microprobe sample lock before analysis.

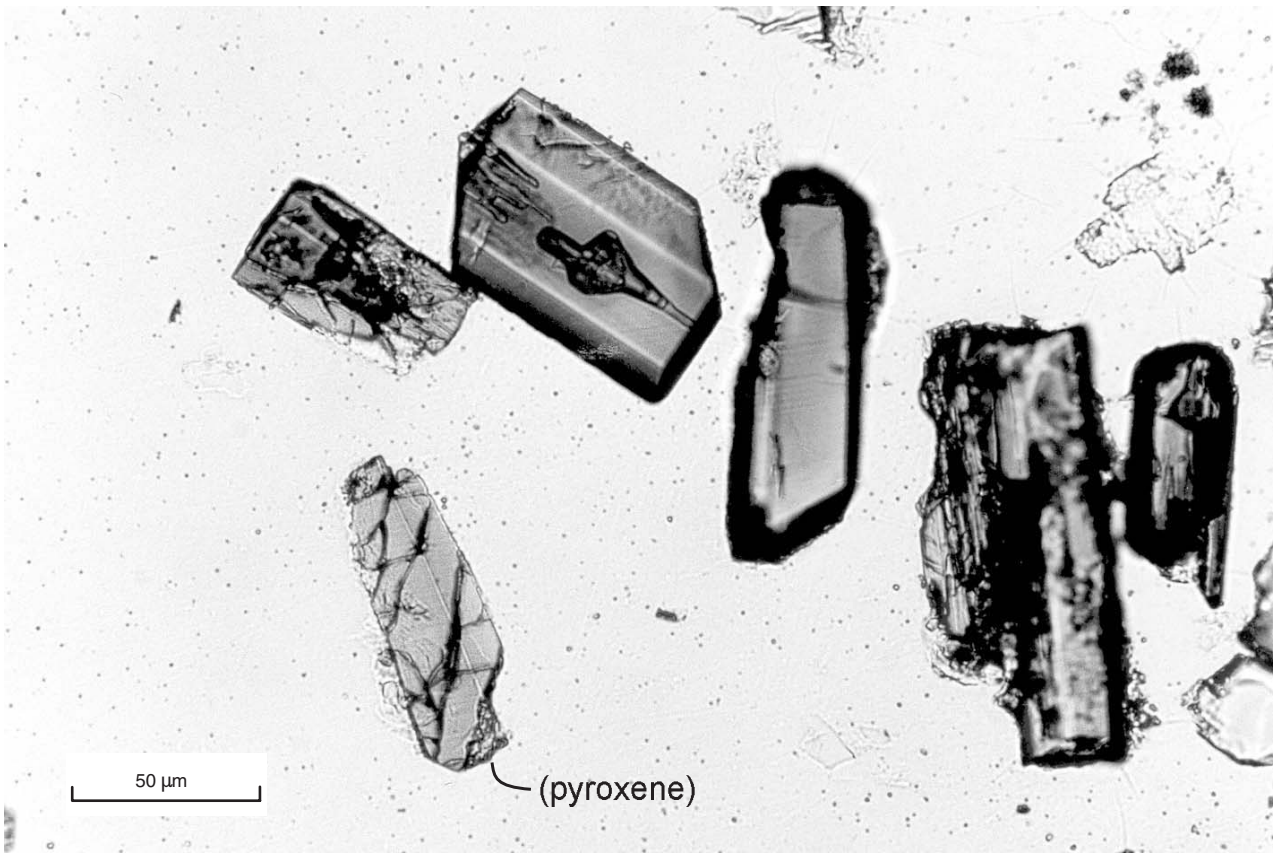

Figure 4. Typical baddeleyite crystals separated from Glenayle Dolerite sample 152661

Measurements of U, Th, and Pb were conducted using the Perth Consortium SHRIMP II ion microprobe at Curtin University of Technology, using operating and data-processing procedures for baddeleyite described by Wingate et al. (1998). Data were collected in sets of six scans through the mass spectrum for both samples during a single analytical session. Calculated ages are based on decay constants recommended by Steiger and Jäger (1977). Values of $^{206}Pb/^{238}U$ measured in baddeleyite by ion microprobe have been shown to vary significantly and systematically with the relative orientation of the baddeleyite crystal structure and the direction of the primary ion beam; therefore, ages are determined from $^{207}Pb/^{206}Pb$ values, which are unaffected by this phenomenon (Wingate et al., 1998; Wingate and Compston, 2000). Accuracy was monitored by repeated analysis of baddeleyite from the 2060 Ma Phalaborwa Carbonatite, which has been characterized previously by both conventional isotope dilution and SHRIMP techniques (Heaman and LeCheminant, 1993; Reischmann, 1995; Wingate, 1997). The mean $^{207}Pb/^{206}Pb$ age of 2063 ± 3.3 Ma (1σ, n = 12, MSWD = 0.14, where σ = standard deviation, n = number of analyses, MSWD = mean square of weighted deviates) is not significantly different from the accepted value (2059.8 ± 0.4 Ma, 1σ), and no corrections for isotope fractionation or hydride interference are indicated. Although subject to high dispersion from crystal orientation effects, $^{238}U/^{206}Pb$ values, determined by calibration against the Phalaborwa Carbonatite baddeleyite, are also reported here for Glenayle Dolerite baddeleyite (Tables 1 and 2, Figs 5a and 6a), and considered semi-quantitatively below as evidence against significant radiogenic-Pb loss in these crystals.

Because of heterogeneity in ^{238}U in the Phalaborwa baddeleyite (a mean value of 300 ppm ^{238}U was assumed, based on previous studies: 292–1389 ppm, Heaman and LeCheminant, 1993; 230–392 ppm, Reischmann, 1995), calculated absolute ^{238}U and ^{232}Th concentrations are approximate, but are proportional to true values within each analytical session. Measured compositions were corrected for common Pb using nonradiogenic ^{204}Pb. Before analysis, each site was cleaned by rastering the primary ion beam over the area for up to three minutes. Subsequently, $^{204}Pb^+$ counts for most analyses remained low and constant, and showed no tendency to decrease over the course of a 15-minute analysis, suggesting that common Pb in these crystals is mainly inherent to the mineral rather than surface related. In most cases corrections are sufficiently small to be insensitive to the choice of common-Pb composition, and an average crustal composition (Cumming and Richards, 1975) appropriate to the age of the mineral was assumed. Weighted mean ages for pooled analyses are reported with 95% confidence intervals (except where noted otherwise), calculated from 1σ uncertainties multiplied by the appropriate value of Student's t for n–1 degrees of freedom.

Table 1. Uranium–lead analytical data for baddeleyite from Glenayle Dolerite sample 152661

Grain area	^{238}U (ppm)	^{232}Th (ppm)	Th/U	f_{206} (%)	$^{206}Pb/^{238}U$ (±1σ)		$^{207}Pb/^{206}Pb$ (±1σ)		$^{207}Pb/^{206}Pb$ age (Ma)	(±1σ)
1.1	366	58	0.16	0.008	0.1897	0.0058	0.07522	0.00268	1 074	70
2.1	218	73	0.34	0.422	0.1621	0.0090	0.07476	0.00347	1 062	91
3.1	201	29	0.15	0.255	0.1914	0.0049	0.07717	0.00273	1 126	69
4.1	67	5	0.08	0.101	0.1719	0.0045	0.07501	0.00149	1 069	39
5.1	71	5	0.08	0.195	0.1680	0.0021	0.07538	0.00235	1 079	61
6.1	139	7	0.05	0.518	0.1851	0.0052	0.07435	0.00120	1 051	32
7.1	73	14	0.19	0.490	0.1750	0.0045	0.07340	0.00215	1 025	58
8.1	222	42	0.19	0.087	0.1785	0.0065	0.07424	0.00119	1 048	32
9.1	192	17	0.09	0.257	0.1806	0.0066	0.07456	0.00179	1 057	48
10.1	238	42	0.18	0.158	0.1634	0.0042	0.07410	0.00184	1 044	49
11.1	364	79	0.22	0.015	0.1871	0.0034	0.07632	0.00109	1 103	28
12.1	137	14	0.11	0.167	0.1854	0.0023	0.07643	0.00176	1 106	45
13.1	50	3	0.07	0.992	0.1805	0.0061	0.07327	0.00734	1 021	190
14.1	226	34	0.15	0.101	0.1751	0.0056	0.07592	0.00096	1 093	25
15.1	192	25	0.13	0.548	0.1687	0.0035	0.07432	0.00115	1 050	31
16.1	242	25	0.10	0.220	0.1824	0.0085	0.07532	0.00276	1 077	72
17.1	111	6	0.05	0.180	0.1742	0.0037	0.07444	0.00129	1 053	35
18.1	172	36	0.21	0.034	0.1719	0.0026	0.07575	0.00199	1 088	52
19.1	94	5	0.05	0.808	0.1664	0.0022	0.07339	0.00177	1 025	48
20.1	59	5	0.08	1.474	0.1729	0.0056	0.07153	0.00405	973	111
21.1	79	8	0.11	1.379	0.1625	0.0034	0.07764	0.00818	1 138	196
22.1	113	14	0.13	2.501	0.1721	0.0045	0.07417	0.00765	1 046	195
23.1	118	9	0.08	1.759	0.2061	0.0053	0.07374	0.00565	1 034	147

NOTES: f_{206} is the proportion of common ^{206}Pb in total measured ^{206}Pb, as determined using $^{204}Pb/^{206}Pb$
Uncertainties in $^{206}Pb/^{238}U$ values do not include a contribution of 4.0% (1σ) arising from calibration against the baddeleyite standard values

Table 2. Uranium–lead analytical data for baddeleyite from Glenayle Dolerite sample 171741

Grain area	^{238}U (ppm)	^{232}Th (ppm)	Th/U	f_{206} (%)	$^{206}Pb/^{238}U$ (±1σ)		$^{207}Pb/^{206}Pb$ (±1σ)		$^{207}Pb/^{206}Pb$ age (Ma)	(±1σ)
1.1	119	25	0.21	0.066	0.1812	0.0066	0.07536	0.00495	1 078	126
2.1	147	14	0.09	0.038	0.1877	0.0050	0.07536	0.00066	1 078	18
3.1	70	6	0.08	0.172	0.1779	0.0024	0.07389	0.00149	1 038	40
4.1	86	2	0.02	0.177	0.1728	0.0038	0.07623	0.00301	1 101	77
5.1	104	15	0.14	0.314	0.1817	0.0022	0.07376	0.00249	1 035	67
6.1	89	12	0.14	0.001	0.1718	0.0044	0.07538	0.00178	1 079	47
7.1	79	7	0.08	0.341	0.1665	0.0046	0.07617	0.00208	1 099	54
8.1	237	37	0.16	0.293	0.1714	0.0043	0.07416	0.00111	1 046	30
9.1	74	3	0.04	0.105	0.1895	0.0045	0.07781	0.00374	1 142	93
10.1	33	3	0.08	1.099	0.1755	0.0033	0.07432	0.00412	1 050	108
11.1	50	5	0.10	0.541	0.1661	0.0033	0.07145	0.00212	970	60
12.1	67	6	0.08	0.475	0.1837	0.0048	0.07274	0.00475	1 007	127
13.1	71	6	0.08	0.412	0.1776	0.0026	0.07666	0.00178	1 112	46
14.1	101	11	0.10	0.412	0.1727	0.0056	0.07304	0.00607	1 015	160
15.1	60	8	0.13	0.630	0.1658	0.0020	0.07352	0.00244	1 028	66
16.1	82	13	0.15	0.344	0.1677	0.0037	0.07653	0.00263	1 109	67
18.1	110	13	0.11	0.550	0.1788	0.0068	0.07439	0.00454	1 052	118
19.1	129	23	0.18	0.585	0.1773	0.0046	0.07593	0.00243	1 093	63
20.1	133	14	0.10	0.371	0.1638	0.0014	0.07351	0.00127	1 028	34
21.1	122	16	0.13	0.415	0.1688	0.0203	0.07546	0.00228	1 081	60
22.1	121	26	0.21	1.368	0.1909	0.0043	0.07404	0.00479	1 043	125
23.1	60	5	0.09	1.020	0.1886	0.0072	0.07654	0.00433	1 109	109
24.1	55	5	0.09	0.608	0.1723	0.0055	0.07308	0.00263	1 016	71

NOTE: f_{206} is the proportion of common ^{206}Pb in total measured ^{206}Pb, as determined using $^{204}Pb/^{206}Pb$
Uncertainties in $^{206}Pb/^{238}U$ values do not include a contribution of 4.0% (1σ) arising from calibration against the baddeleyite standard values

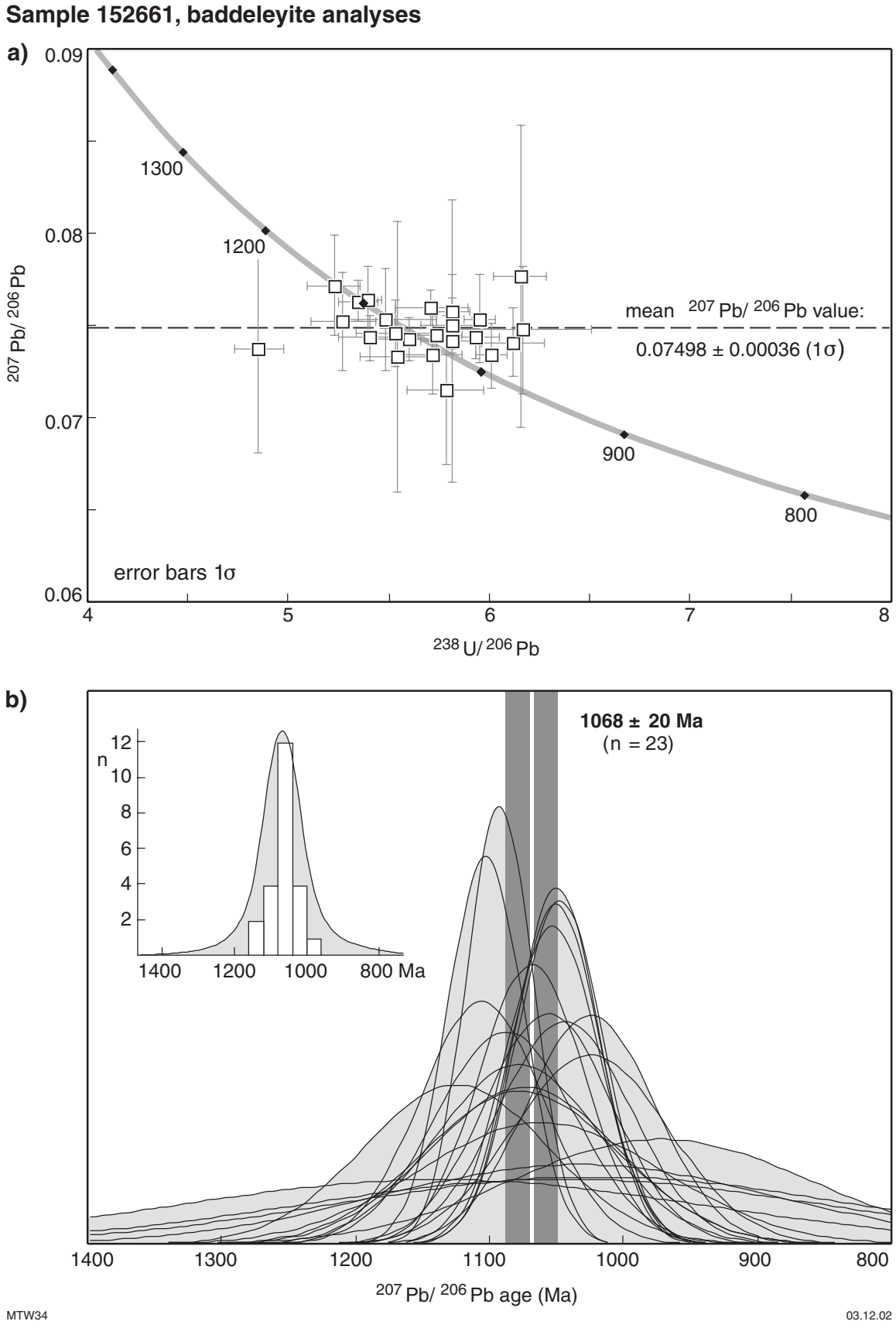

Figure 5. Ion microprobe analytical data for baddeleyite from sample 152661: a) U–Pb evolution (concordia) diagram; b) Normalized probability density curves for individual $^{207}Pb/^{206}Pb$ values. Dark-grey bands indicate the weighted mean age and 95% confidence interval. Inset shows the cumulative probability density curve and histogram of all $^{207}Pb/^{206}Pb$ ages; n = number of analyses

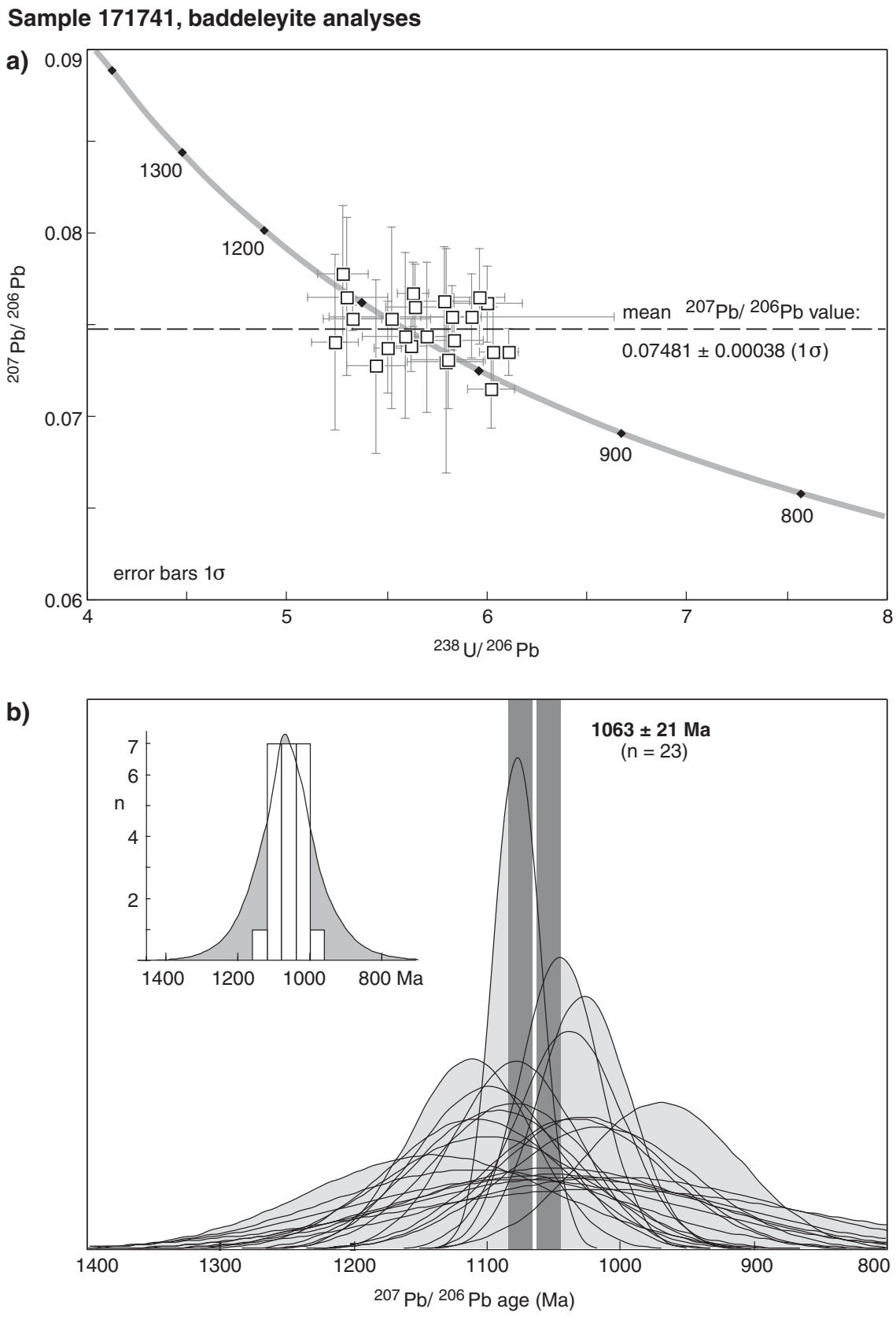

Figure 6. Ion microprobe analytical data for baddeleyite from sample 171741: a) U–Pb evolution (concordia) diagram; b) Normalized probability density curves for individual $^{207}Pb/^{206}Pb$ values. Dark-grey bands indicate the weighted mean age and 95% confidence interval. Inset shows the cumulative probability density curve and histogram of all $^{207}Pb/^{206}Pb$ ages; n = number of analyses

Results

Sample 152661, east of site D

This sample of fresh, medium-grained granophyric dolerite was collected 1.1 km east of palaeomagnetism site D, in part of the same intrusion from which the palaeomagnetic samples were collected (Fig. 3). Twenty-three analyses were conducted of 23 baddeleyite crystals (Table 1). Concentrations of ^{238}U range from 50 to 366 ppm, with a median of 140 ppm; ^{232}Th ranges from 3 to 80 ppm, with a median of 14 ppm; Th/U varies from 0.05 to 0.3, with a median of 0.1. Common Pb is low for most analyses. The proportion of common ^{206}Pb in total measured ^{206}Pb (f_{206} in data tables) ranges from less than 0.01 to 1.0% for 19 analyses, and is between 1.0 and 2.5% for the remaining four analyses.

All 23 $^{207}Pb/^{206}Pb$ values agree to within analytical precision (Fig. 5), yielding a mean of 0.07498 ± 0.00036 (MSWD = 0.4), equivalent to an age of 1067.9 ± 9.6 Ma (1σ). No significant correlation exists between $^{207}Pb/^{206}Pb$ and U or Th concentration. Large uncertainties for several analyses reflect low U content (and therefore low radiogenic Pb) and large relative corrections for common Pb (Table 1). The weighted mean $^{207}Pb/^{206}Pb$ age of 1068 ± 20 Ma (95% confidence interval) is interpreted as the age of baddeleyite crystallization.

Sample 171741, site K

This sample of medium-grained granophyric dolerite was collected at palaeomagnetism site K, from the same outcrop area as the palaeomagnetic samples (Fig. 3). Twenty-three baddeleyite crystals were analysed (Table 2). Concentrations of ^{238}U range from 33 to 237 ppm, with a median of 86 ppm; ^{232}Th ranges from 2 to 37 ppm, with a median of 10 ppm; Th/U varies between 0.02 and 0.2. Values for f_{206} range from less than 0.01 to 0.6% for 20 analyses, and are between 1.0 and 1.4% for the remaining three analyses.

Twenty-three $^{207}Pb/^{206}Pb$ values agree to within analytical precision (Fig. 6), with a mean of 0.07481 ± 0.00038 (MSWD = 0.4), equivalent to an age of 1063.4 ± 10.3 Ma (1σ). Large uncertainties correlate with either large corrections for common Pb or low U content, or both (Table 2). The weighted mean $^{207}Pb/^{206}Pb$ age of 1063 ± 21 Ma (95% confidence interval) is considered the best estimate of the age of baddeleyite crystallization.

Discussion and summary

Baddeleyite crystals were recovered from two samples of Glenayle Dolerite and dated by SHRIMP. Ages based on $^{207}Pb/^{206}Pb$ values for the two samples agree to within analytical precision (Table 3). Low dispersion of $^{207}Pb/^{206}Pb$ values implies that any loss of radiogenic Pb was insignificant, or was geologically recent in age. This inference is supported by values of $^{238}U/^{206}Pb$ for each sample, which (although subject to bias arising from crystal orientation effects) as a group are centred approximately on concordia (Figs 5a, 6a), rather than being mainly normally discordant, as would be expected in the case of significant lead loss.

Table 3. Mean $^{207}Pb/^{206}Pb$ ages for Glenayle Dolerite samples

Site	*Sample*	*Mineral dated*	*n*	*Mean $^{207}Pb/^{206}Pb$ age (Ma)*
D	152661	baddeleyite	23	1068 ± 20
B	171741	baddeleyite	23	1063 ± 21
Mean of two samples			46	1066 ± 14

NOTES: n = number of analyses. Ages are reported with 95% confidence intervals

It is very unlikely that baddeleyite in mafic intrusions can be inherited from older rocks, hence the ages obtained for the two samples are considered to date accurately the time of crystallization of the dolerite. As discussed above (**Geological setting**), it is likely that the two dated samples are comagmatic, perhaps part of the same sill. It is therefore reasonable to combine all 46 analyses from two samples to yield a mean $^{207}Pb/^{206}Pb$ age of 1066 ± 14 Ma (95% confidence interval), which is interpreted as the best estimate of the age of the Glenayle Dolerite.

Palaeomagnetism

In this section palaeomagnetic results are reported for Glenayle Dolerite sills intruding the Salvation Group on the STANLEY and southwestern TRAINOR 1:250 000 map sheets, and for a sill (Prenti Dolerite) intruding the Earaheedy Group on the KINGSTON 1:250 000 map sheet. Magnetic minerals (mainly Fe–Ti oxides) within an igneous rock record the direction of the magnetic field at the time the rock cools. Dolerite dykes and sills, within which the typical primary magnetic carrier is relatively pure magnetite (Fe_3O_4), are excellent recorders of the Earth's magnetic field. Fine-grained (single-domain, SD) magnetite, which is present in chilled sill margins, is highly stable and resistant to later thermal resetting of its magnetization. In the laboratory detailed thermal (TH) and alternating field (AF) demagnetization techniques are used to progressively remove less stable magnetic components in order to isolate a 'characteristic' remanence. Within a single crustal block all rocks of the same age (within a few million years) would be expected, in the absence of later alteration or deformation, to yield similar palaeomagnetic poles, hence palaeomagnetism can be used to correlate rock units over wide areas.

Sample collection

Core samples of Glenayle Dolerite were collected at nine sites (A to J, Fig. 3; adjacent sites F and G are combined as a single site) using a portable diamond drill, and at one site (K) by collecting oriented block samples from which cores were drilled in the laboratory. Core samples

were also drilled at a single site in the Prenti Dolerite of the Earaheedy Basin. Site descriptions are provided in Appendix 1. Geographic site coordinates were determined using a Global Positioning System (GPS) receiver. Between five and twelve cores (typically seven to nine), separated by up to several tens of metres, were drilled at each site. To avoid possible effects of lightning strikes, samples were obtained mainly from low-lying areas, such as creek beds, where the least weathered rocks also tend to be present. Core samples were oriented using both magnetic and sun compasses. For the majority of samples, magnetic and sun orientation measurements agree to within 5°; in all cases, sun readings were taken as accurate. All Glenayle Dolerite samples are relatively fresh and unaltered; the outcrop sampled in the Prenti Dolerite (site L) is moderately weathered.

Because the dolerite sills are commonly flat lying and the topography is subdued, bedding attitudes in adjacent sedimentary rocks could not be measured at all sites, but were estimated in most cases from detailed regional mapping of sedimentary outcrops within a few kilometres of each site (Pirajno and Hocking, 2001, 2002). Tectonic corrections of up to 5° were applied to data from four of 11 sites (Table 4).

Analytical methods

Palaeomagnetic analyses were conducted at the University of Western Australia laboratory in Perth. Each core sample, 2.5 cm in diameter and typically between 3 and 8 cm in length, was cut into 2.2 cm-long specimens for analysis. Remanence composition was determined by detailed stepwise AF demagnetization (up to 18 steps, up to 160 mT) of one specimen from each core, using a 2G-Enterprises cryogenic magnetometer. Up to four specimens from each site were subjected to detailed stepwise thermal demagnetization (up to 11 steps, 100 to 580°C), using a Magnetic Measurements thermal demagnetizer and 2G-Enterprises magnetometer. Samples were pretreated in four steps up to 20 mT before thermal analysis to reduce possible isothermal remanence (IRM) due to lightning strikes (Schmidt, 1993). To monitor possible mineralogical changes during heating, magnetic susceptibility was measured in selected samples after each heating step using a Bartington MS2 susceptibility meter. Magnetic mineralogy was investigated from thermal demagnetization characteristics and, in selected samples, from detailed variation of susceptibility versus temperature (20 to 700°C) obtained using the Bartington meter in conjunction with an automated Bartington furnace. Magnetization vectors were isolated using Principal Component Analysis (Kirschvink, 1980). Line segments were calculated with a minimum of four data points and a maximum angular deviation (MAD) of 10 to 15°. The AF and thermal results for specimens from the same core sample were averaged and sample means given unit weight in statistical calculations for each site.

Results

Measurements were conducted on 109 specimens from 86 core samples. Natural remanent magnetizations (NRMs) are of moderate intensity, between 0.1 and 48 A/m, with an average of about 7 A/m (Fig. 7). For the majority of specimens a low-coercivity overprint was removed by AF demagnetization to 10 or 20 mT. Directions are consistent for specimens from the same core sample, but, in most cases, vary randomly for different samples. These overprints probably have a variety of origins, including weathering and lightning. Some are similar to Earth's present field direction, and may be recent viscous remanent magnetizations (VRMs).

After removal of low-coercivity overprints, magnetizations are typically single component, and vector endpoints decay linearly to the origin in orthogonal plots, yielding well-defined directions (Figs 8 and 9). Thermal and AF demagnetization methods yield similar

Table 4. Site mean directions and virtual geomagnetic poles (VGPs) for the Glenayle Dolerite (sites A to K) and Prenti Dolerite (site L)

Site	*Location*		*Bedding*	*N, n*	*Direction (in situ)*				*Direction (rotated)*		*VGP*	
	Lat. (S)	*Long. (E)*	*(dip/dip azimuth)*		*D (°)*	*I (°)*	*k*	a_{95} *(°)*	*D' (°)*	*I' (°)*	*Lat. (N)*	*Long. (E)*
A	25°25'16"	122°14'53"	02/035	9, 7	345.3	43.8	99	6.1	346.7	42.5	37°	105°36'
B	25°1'12"	121°35'10"		9, 6	333.4	49.6	75	7.8	333.4	49.6	29°	95°24'
C	25°4'55"	121°42'54"		11, 8	345.3	40.6	85	6.0	345.3	40.6	39°42'	104°6'
D	25°11'35"	121°53'17"		16, 10	346.5	36.2	190	3.5	346.5	36.2	42°48'	104°30'
E	25°5'28"	122°0'54"		9, 6	340.2	52.4	446	3.2	340.2	52.4	28°54'	103°6'
FG	25°11'38"	122°13'30"	05/005	15, 8	344.6	61.4	90	5.9	347.3	56.7	26°24'	111°
H	25°13'52"	122°32'17"		7, 5	357.1	61.4	109	7.4	357.1	61.4	22°12'	120°12'
I	25°12'47"	122°29'2"		12, 8	005.0	57.7	208	3.9	005.0	57.7	26°18'	126°54'
J	25°16'34"	122°5'53"	05/035	8, 6	336.4	51.2	38	11.0	341.3	48.4	32°30'	102°42'
K	24°55'41"	121°36'22"		6, 6	356.1	49.7	15	17.9	356.1	49.7	34°24'	117°30'
L	26°31'37"	122°49'26"	04/035	7, 4	346.1	42.3	34	16.0	348.7	39.6	39°48'	109°12'

NOTES: N = number of specimens analysed
D = declination (east of north)
k = Fisher's (1953) precision parameter
VGPs are calculated from rotated (bedding-corrected) directions
n = number of samples given unit weight in calculation of site mean direction
I = inclination (positive downwards)
α_{95} = circle of 95% confidence about mean direction

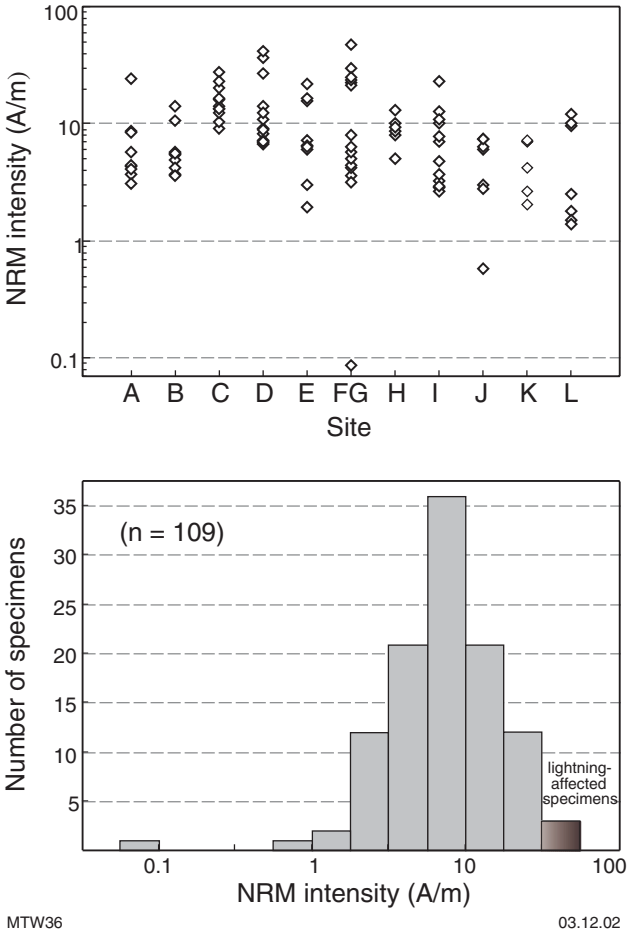

Figure 7. Natural remanent magnetization (NRM) intensities measured in samples from the Glenayle Dolerite (sites A–K) and Prenti Dolerite (site L). Adjacent sites F and G are combined as a single site; n = number of analyses

results. Unblocking temperatures of between 500 and 580°C, in most cases above 540°C, indicate that relatively pure magnetite is the dominant remanence carrier. Most specimens are stable during AF treatment up to fields of 60 to 160 mT. A range of AF demagnetization characteristics indicates variable proportions of multi-domain (MD) and single-domain grains, the latter exhibiting characteristic sigmoidal AF decay curves (e.g. Figs 8a and 9a). These observations are corroborated by detailed susceptibility versus temperature measurements, which indicate Curie temperatures of above 530°C and the presence of SD magnetite (Fig. 10).

Aberrant palaeomagnetic directions measured in six samples from suspected rotated blocks at four sites, and in three high-intensity samples probably affected by lightning, were not considered in the calculation of site mean directions (Fig. 11). All nine excluded directions are significantly different from the site mean direction at 99% confidence level (McFadden, 1982). One sample became unstable at 20 mT and yielded no useful information. The remaining palaeomagnetic directions at each site are directed consistently to the north or north-northwest with moderate downward inclination, and low within-site dispersion (Fig. 11). After applying corrections for bedding tilt to data from three of ten sites, the concentration parameter, k, increases from 62 to 69 (Fig. 12). The mean palaeomagnetic direction for sites A to K in the Glenayle Dolerite, after tectonic correction, is D = 347.3°, I = 49.8° (α_{95} = 5.9°, n = 10 sites), where D = declination (east of north); I = inclination (positive downwards); α_{95} = circle of 95% confidence about mean direction; k = Fisher's (1953) precision parameter; n = number of sites.

Similar results were obtained from four of seven samples from site L in the Prenti Dolerite (Fig. 13). The mean direction (square symbol in Fig. 12), after recalculation to correspond to that expected in the centre of the Glenayle area (25°12'S, 122°5'E), is in excellent agreement with directions observed in the Glenayle Dolerite. Three discordant directions at site L (Fig. 13) may reflect low-temperature chemical overprints related to the moderate weathering that has affected the outcrop.

Evidence supporting a primary origin for the Glenayle magnetization includes:

- low within-site dispersion, which is typical of primary thermoremanent magnetizations (TRM) observed in intrusions that cool rapidly;
- SD magnetite grains in some samples, which require heating close to 580°C to unblock their magnetization (Pullaiah et al., 1975; Walton, 1980), and the lack of evidence for a younger thermal event that could have caused a remagnetization;
- precise agreement between the tilt-corrected mean direction for the Glenayle Dolerite and the primary magnetic remanence (star in Fig. 12) observed in dolerite sills of the same age, 600 km to the west, on the Edmund 1:250 000 map sheet (Fig. 1; Wingate, 2002).

These observations indicate that the magnetization of the Glenayle Dolerite is a primary TRM dating from the time of sill emplacement at 1066 Ma.

The pole position, GLD, for ten sites (A to K) in the Glenayle Dolerite, calculated as the mean of site virtual geomagnetic poles (VGPs, Table 4), lies at 32°18'N, 122°17'E (A_{95} = 6.3°, n = 10 sites, where A_{95} = radius of circle of 95% confidence about mean pole). Including the VGP from the Prenti Dolerite (site L) changes the pole position slightly, to 33°N, 109°17'E (A_{95} = 5.8°, n = 11 sites). This result meets six of the maximum seven criteria for a fully reliable palaeopole, according to the scheme of Van der Voo (1990). Because of the small number of separate intrusions sampled (probably two to four), however, the GLD pole may not have adequately averaged palaeosecular variation (PSV), and should therefore be regarded as a virtual geomagnetic pole (VGP).

Summary

Palaeomagnetic measurements were conducted on samples from 10 sites (A–K, Fig. 3) in the Glenayle Dolerite,

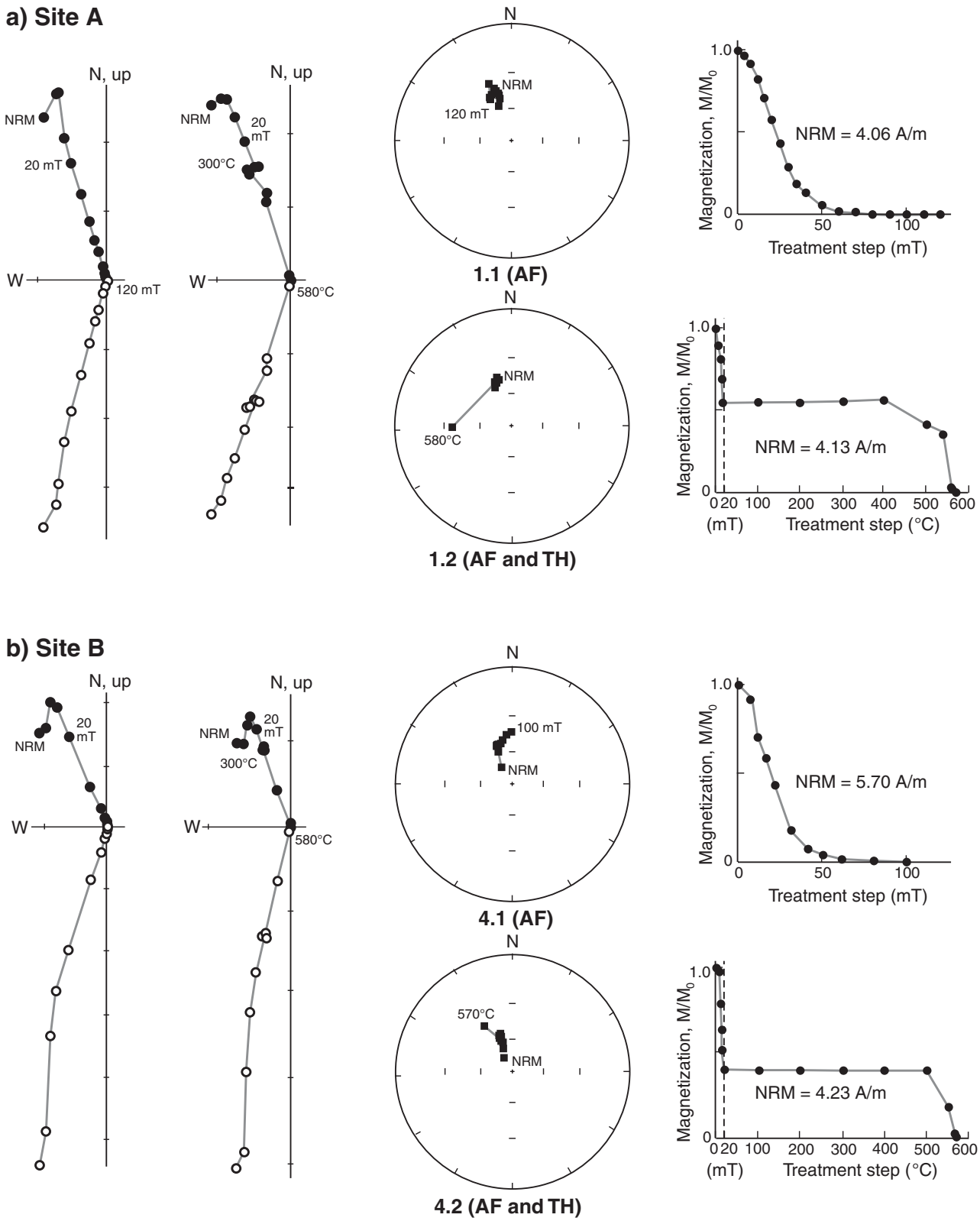

Figure 8. Examples of alternating field (AF) and thermal (TH) demagnetization of two samples of a single core from each of sites A and B. Orthogonal projections show trajectories of vector endpoints during progressive demagnetization (open/closed symbols represent vertical/horizontal planes). Closed symbols in lower hemisphere equal-angle stereographic projections indicate downward pointing directions. Demagnetization curves show changes in magnetization intensity during treatment. Reference frame is present horizontal. The natural remanent magnetization (NRM) intensity is the initial intensity measured before demagnetization

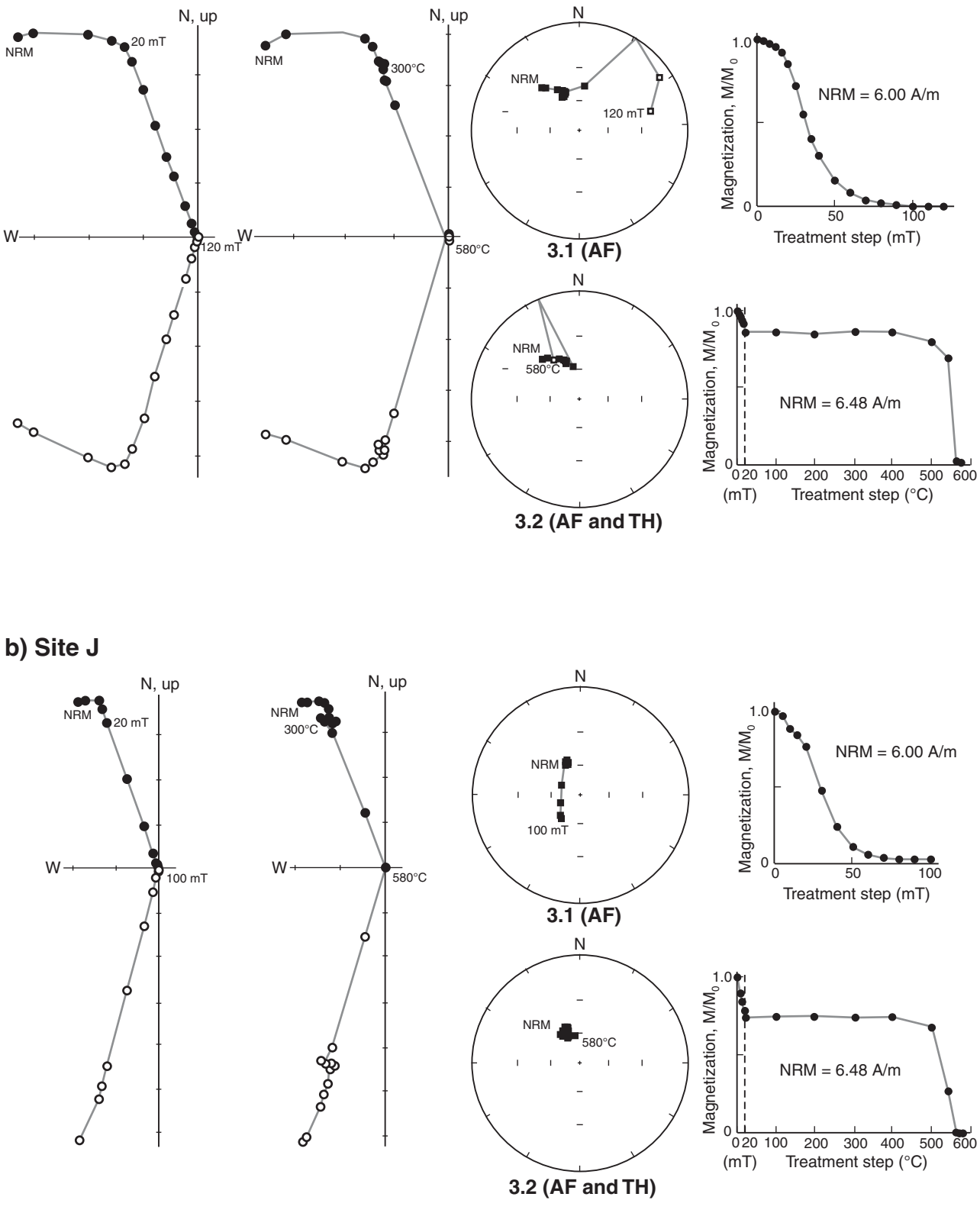

MTW38

18.11.02

Figure 9. Examples of alternating field (AF) and thermal (TH) demagnetization of two samples of a single core from each of sites E and J. Orthogonal projections show trajectories of vector endpoints during progressive demagnetization (open/closed symbols represent vertical/horizontal planes). Closed symbols in lower hemisphere equal-angle stereographic projections indicate downward pointing directions. Demagnetization curves show changes in magnetization intensity during treatment. Reference frame is present horizontal. The natural remanent magnetization (NRM) intensity is the initial intensity measured before demagnetization

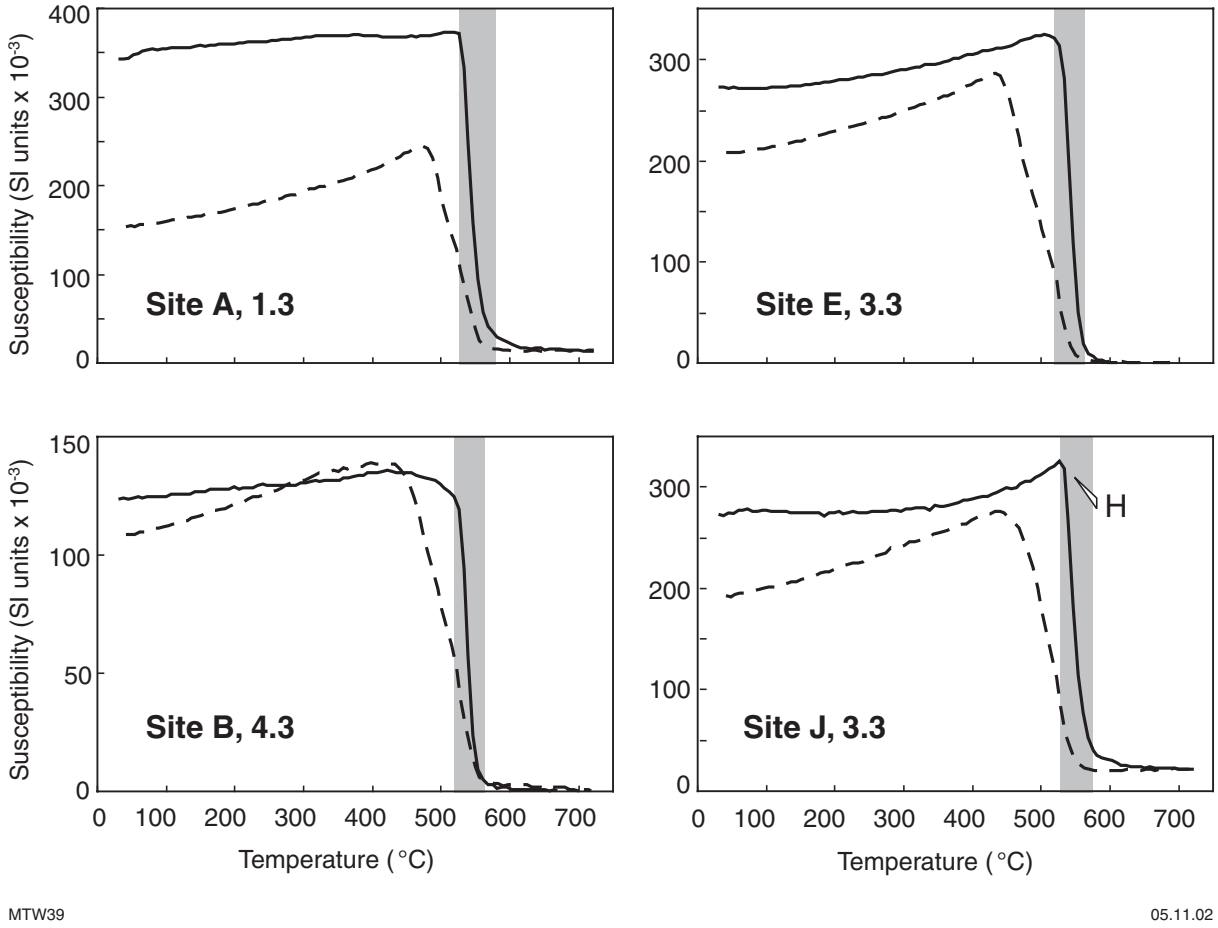

Figure 10. Variation of low-field susceptibility with temperature for the four samples shown in Figures 8 and 9 (heating = solid curves; cooling = dashed curves). In each case, magnetizations are unblocked within a narrow temperature interval (shaded) between 520 and 580°C. The sharp increase in susceptibility (H, Hopkinson peak) just before unblocking indicates the presence of fine-grained (single-domain, SD) magnetite. Lower susceptibilities during cooling indicate that some magnetite was consumed (probably oxidized to hematite) above 580°C

which intruded the Salvation Group, and one site (L) in the Prenti Dolerite sill, which intruded the Earaheedy Group (Fig. 1). After removal of low-stability overprints, the majority of samples from all sites exhibits a single stable magnetization component directed to the north or north-northwest with moderate downwards inclination. Palaeomagnetic directions measured in samples from the Prenti Dolerite are indistinguishable from those in the Glenayle Dolerite. Based on rock magnetic and palaeomagnetic characteristics, and on agreement with primary palaeomagnetic directions in dolerites of the same age in the western Bangemall Supergroup (Wingate, 2002), the Glenayle and Prenti Dolerite magnetizations are inferred to have been acquired during sill emplacement and cooling at c. 1070 Ma. Combining virtual geomagnetic poles for 11 sites (A to L) in the Glenayle and Prenti Dolerites yields a mean pole position at 33°N, 109°17'E (Table 5). The sampled dolerites probably represent an insufficient number of separate intrusions, however, to have adequately averaged palaeosecular variation of the Earth's magnetic field.

Synthesis

Age of the Glenayle Dolerite and Salvation Group

The SHRIMP baddeleyite ages of 1068 ± 20 and 1063 ± 21 Ma obtained during this study are interpreted as accurate estimates of the time of crystallization of the Glenayle Dolerite. In view of the likelihood that the two U–Pb samples were collected from parts of the same intrusion, the baddeleyite data are combined to yield a mean age of 1066 ± 14 Ma (95% confidence limits), which is regarded as the best estimate of the age of the Glenayle Dolerite magmatic event. The age of 1066 Ma is also a minimum age for deposition of the Salvation Group, and rules out any correlation with Neoproterozoic rocks of the Sunbeam Group.

Recent K–Ar geochronology suggests minimum ages for crystallization of the Glenayle Dolerite of 968 and 917 Ma (Nelson, 2002). These ages are significantly younger than those determined from baddeleyite,

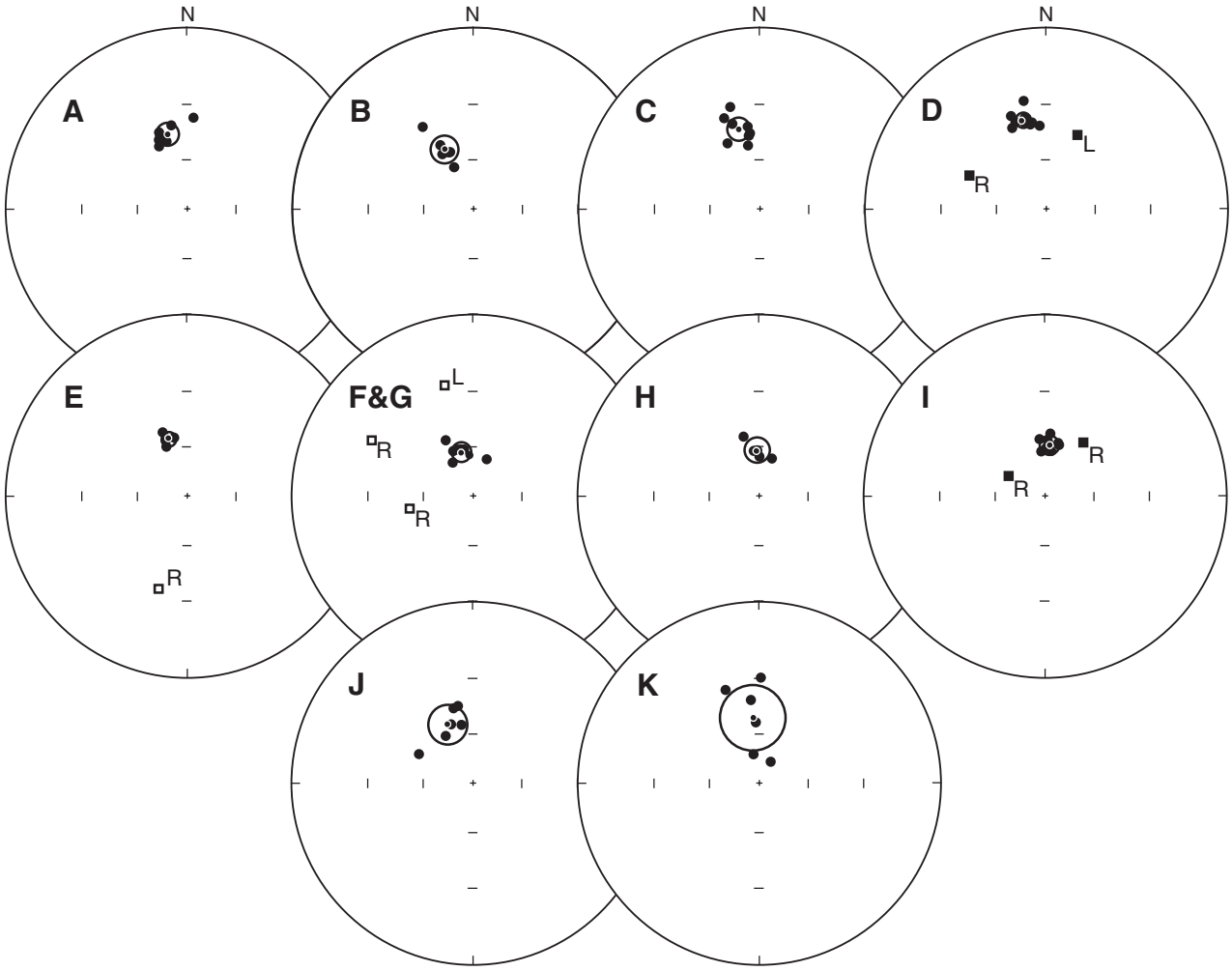

Figure 11. Equal-angle stereographic projections showing palaeomagnetic directions at sites A to K in the Glenayle Dolerite. Site mean directions are shown by small symbols and a_{95} confidence circles (a_{95} = circle of 95% confidence about mean direction). Closed symbols indicate downward pointing directions in lower hemisphere. Reference frame is present horizontal. Square symbols indicate results not included in calculation of site mean directions (L = lightning-affected samples; R = sample from suspected rotated block)

suggesting that the K–Ar samples have experienced some loss of radiogenic Ar.

Regional correlations

The SHRIMP baddeleyite age of 1066 ± 14 Ma obtained for the Glenayle Dolerite is within uncertainty of the SHRIMP baddeleyite and zircon age of 1070 ± 6 Ma reported by Wingate (2002) for dolerite sills intruding the Edmund and Collier Groups in the western part of the Bangemall Supergroup. This implies that the mafic rocks in the two areas were emplaced during the same magmatic event. This conclusion is corroborated by the close correspondence of palaeomagnetic directions (Fig. 12) and poles (Fig. 14) for the Glenayle Dolerite and western Bangemall Supergroup dolerites.

The tilt-corrected mean palaeomagnetic direction measured in the Prenti Dolerite at site L (Fig. 13) in the Earaheedy Basin, recalculated for the centre of the Glenayle Dolerite sampling area (25°12'S, 122°5'E), is indistinguishable from the mean Glenayle Dolerite direction (Fig. 12), implying that the intrusions in the two areas are similar in age and were probably emplaced during the same event at c. 1070 Ma. This is supported by Rb–Sr and K–Ar ages of c. 1050 Ma reported for dolerite sills in the Earaheedy Basin by Compston (1974) and Preiss et al. (1975).

A K–Ar age of 1058 ± 13 Ma was obtained for basalt at the base of drillhole GSWA Empress 1A in the western Officer Basin (Stevens and Apak, 1999), and U–Pb ages averaging about 1075 Ma were determined for mafic intrusive rocks of the Giles Complex in the western Musgrave Complex (Glikson et al., 1996). Dolerite dykes that trend east-northeasterly across the northwest Yilgarn Craton (part of the Muggamurra swarm of Myers et al., 1996) have yielded a preliminary SHRIMP U–Pb

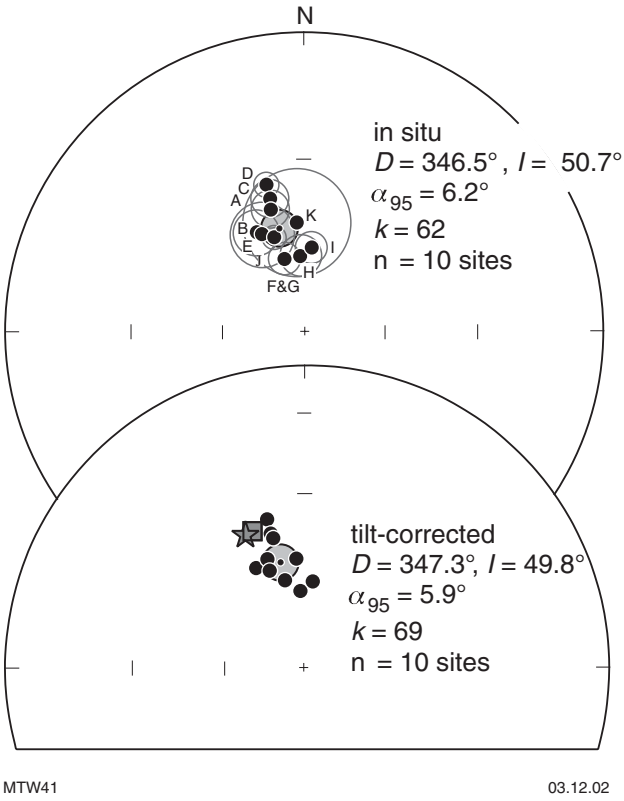

Figure 12. Site mean directions for Glenayle Dolerite, in geographic (in situ) and stratigraphic (tilt-corrected) coordinates. The overall mean direction in each case is shown by a small symbol and shaded a_{95} circle. Also shown are palaeomagnetic directions expected at the centre of the Glenayle study area (25°12'S, 122°5'E) for 1070 Ma sills (Wingate, 2002) in the western Bangemall Supergroup (star) and for the Prenti Dolerite sill intruding the Earaheedy Group at site L (square). Closed symbols indicate downward pointing directions in lower hemisphere. *D* = declination (east of north); *I* = inclination (positive downwards); α_{95} = semi-angle of cone of 95% confidence about mean direction; *k* = Fisher's (1953) precision parameter; n = number of sites

age of about 1070 Ma (Wingate, M. T. D., unpublished data). Late Mesoproterozoic (c. 1070 Ma) mafic igneous rocks therefore outcrop, with an east-southeasterly trend, from the western margin of Western Australia to the Musgrave Complex, over a distance of at least 1200 km (Fig. 15). This observation prompted Pirajno et al. (2002) to suggest that these mafic rocks might represent a single large igneous province (LIP). The 1090 ± 32 Ma Alcurra dyke swarm (Kulgera sills) of the eastern Musgrave Complex, and possibly the 1076 ± 33 Ma Stuart dykes of the southern Arunta Orogen (Sm–Nd isochron ages; Zhao and McCulloch, 1993), may also be related to this event.

It is possible, particularly in LIPs, for basaltic magma to flow horizontally for hundreds or thousands of kilometres through the crust (Ernst and Baragar, 1992; White, 1992), hence the Glenayle Dolerite magma could have originated from a source either beneath or perhaps outside the Edmund and Collier Basins. Moreover, a single intrusion could extend through the entire Edmund and Collier Basins — a distance of at least 900 km. This could be explored further by studying the magnetic fabrics (anisotropy of magnetic susceptibility; Tarling and Hrouda, 1993) of the mafic igneous rocks, which can be used to infer magma flow directions (e.g. Ernst and Baragar, 1992).

Implications for regional tectonics

Dolerite emplacement at 1070 Ma in the Bangemall Supergroup and surrounding rocks occurred during a period of major extension, and may represent the final phase of formation of the Collier Basin. In the western part of the Bangemall Supergroup, Wingate (2002) suggested that this extension was oriented northeast–southwest, roughly orthogonal to the basin axis. Extension in the southeast Collier Basin was presumably oriented in a similar direction, approximately orthogonal to the southern margin of the basin, which coincides roughly with the northern margin of the Yilgarn Craton. The agreement of palaeomagnetic directions from the Glenayle

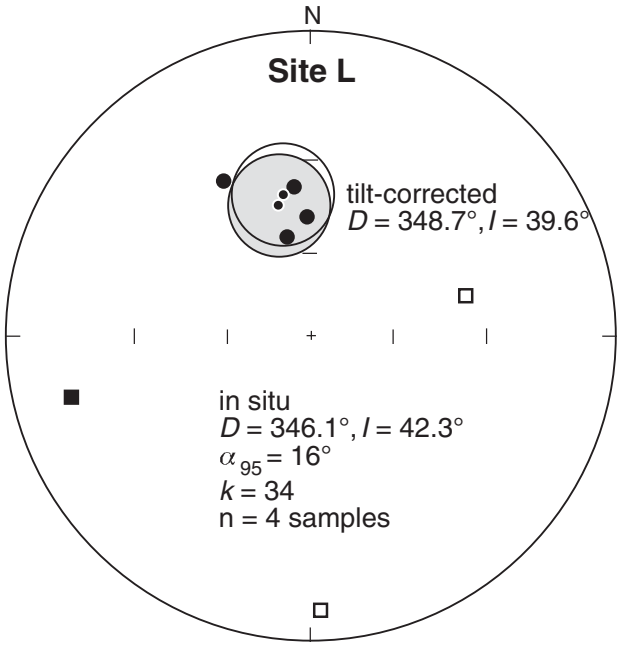

Figure 13. Equal-angle stereographic projection showing palaeomagnetic directions, uncorrected for bedding tilt, at site L in the the Prenti Dolerite. The site mean directions (in situ and tilt-corrected) are shown by small symbols and a_{95} confidence circles. Square symbols indicate three results from weathered rocks that were not included in calculation of the site mean direction. Open/closed symbols indicate upward/downward pointing directions in lower hemisphere. *D* = declination (east of north); *I* = inclination (positive downwards); α_{95} = semi-angle of cone of 95% confidence about mean direction; *k* = Fisher's (1953) precision parameter; n = number of sites

Table 5. Mean palaeomagnetic directions and poles for the Glenayle and Prenti Dolerites, and western Bangemall Supergroup dolerites

		Mean direction					Pole position				
		n	*D* (°)	*I* (°)	*k*	α_{95}	*n*	Lat. (N)	Long. (E)	*k*	A_{95}
1	Glenayle Dolerite (GLD), in situ	10	346.5	50.7	62	6.2	–	–	–	–	–
2	GLD, tilt-corrected	10	347.3	49.8	69	5.9	10	32°18'	109°18'	59	6.3
3	GLD + Prenti Dolerite	–	–	–	–	–	11	33°	109°18'	62	5.8
4	western Bangemall sills (BBS; Wingate, 2002)	–	–	–	–	–	11	33°48'	95°	32	8.3
5	GLD + Prenti Dolerite + BBS (see text)	–	–	–	–	–	13	34°18'	97°12'	34	7.3

NOTES: n = number of sites
D = declination (east of north)
I = inclination (positive downwards)
k = Fisher's (1953) precision parameter
α_{95} = circle of 95% confidence about mean direction
A_{95} = radius of circle of 95% confidence about mean pole
Pole positions for GLD and GLD + Prenti Dolerite are the means of virtual geomagnetic poles (VGPs) in Table 4. VGPs are calculated from rotated (bedding-corrected) directions

Dolerite, Prenti Dolerite, and western Bangemall Supergroup dolerites (Fig. 12) indicates that no significant vertical axis rotations occurred within the Edmund and Collier Groups or surrounding rocks since at least 1070 Ma.

Widespread magmatism across western and central Australia at 1090–1060 Ma (Fig. 15) was synchronous with deformation and magmatism in the Pinjarra Orogen (Harris, 1995; Bruguier et al., 1999). Wingate (2002) proposed that the Edmundian Orogeny, which affected the western Edmund and Collier Basins, may have occurred soon after dolerite emplacement at 1070 Ma. This suggestion is based on:

- the observation that the Edmund Fold Belt corresponds with the area of greatest concentration of dolerite sills;
- the likelihood that dolerite emplacement would have involved advection of considerable heat and consequent thermal weakening of the crust;
- the presence of a possible source of compressive stress during 1090–1060 Ma events in the adjacent Pinjarra Orogen.

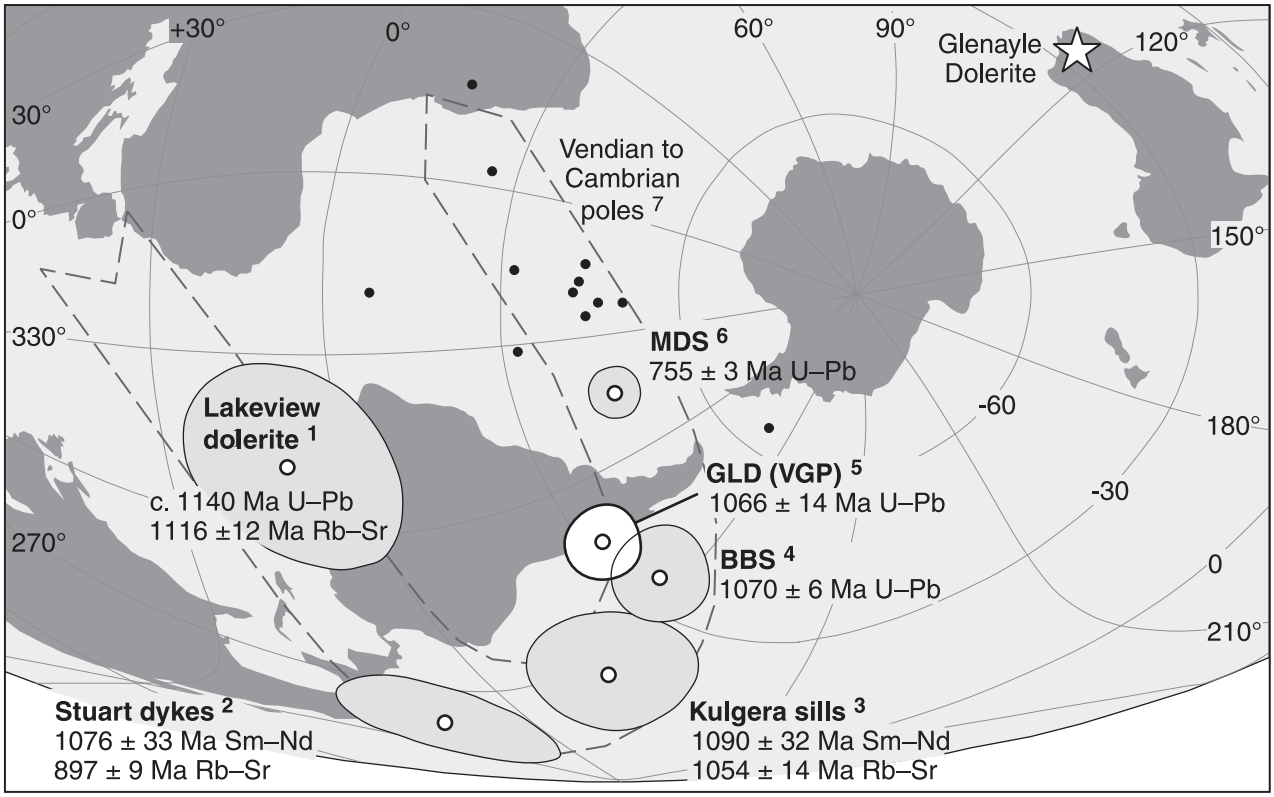

Figure 14. Late Mesoproterozoic to Early Cambrian south palaeopoles for Australia (after Wingate, 2002). GLD = Glenayle Dolerite; BBS = western Bangemall sills; MDS = Mundine Well dyke swarm. A_{95} confidence circles are shown for the MDS and older poles; A_{95} = radius of circle of 95% confidence about mean pole. Sources: 1 = Tanaka and Idnurm (1994); 2 = Idnurm and Giddings (1988); 3 = Camacho et al. (1991); 4 = Wingate (2002); Wingate et al. (2002); 5 = this study; 6 = Wingate and Giddings (2000); 7 = compilation in Wingate and Giddings (2000)

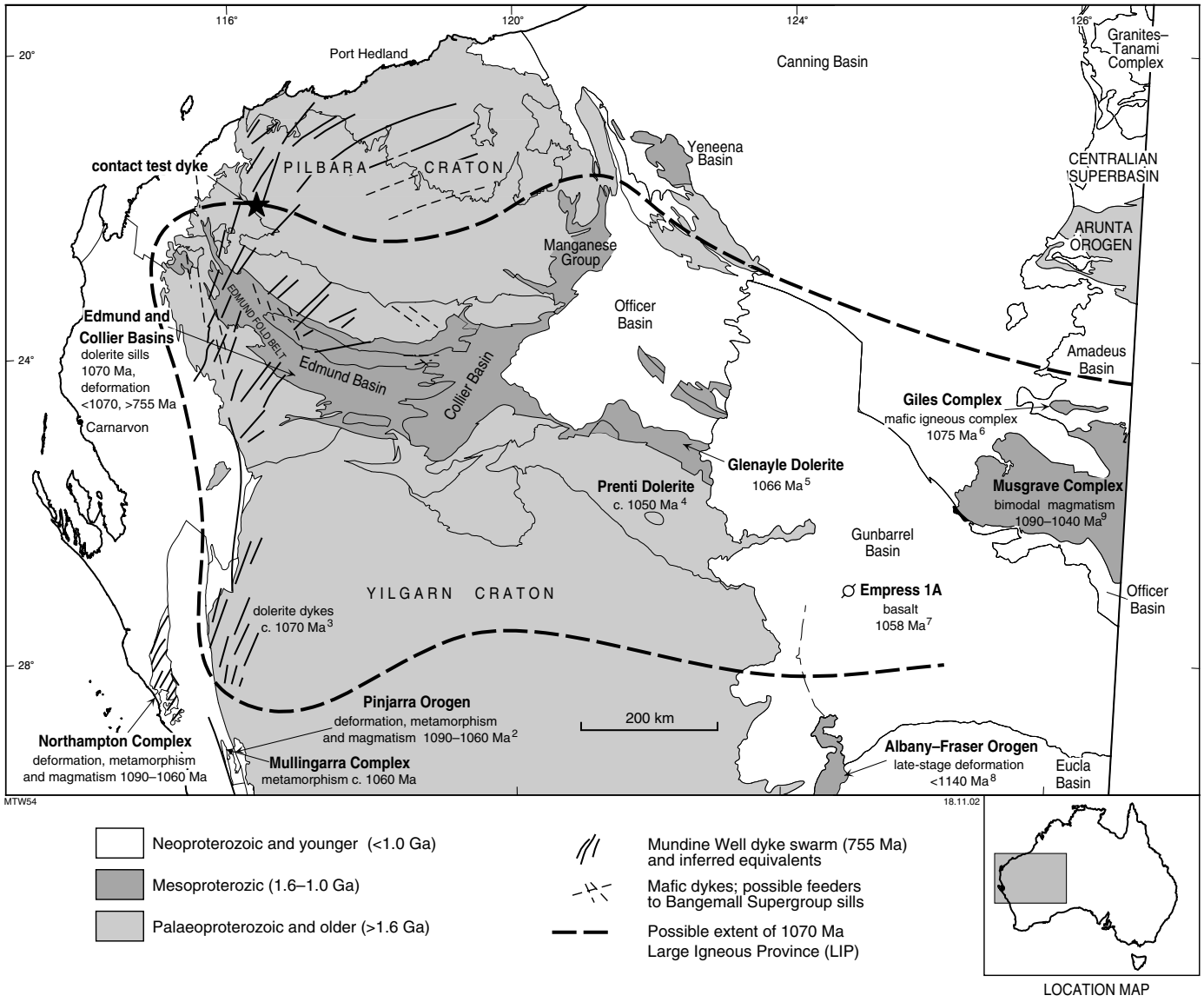

Figure 15. Late Mesoproterozoic (c. 1070 Ma) events in the western part of Australia. The heavy dashed line shows the possible extent of a proposed 1070 Ma large igneous province (LIP). Sources: 1 = Wingate (2002); 2 = Bruguier et al. (1999); 3 = M. T. D. Wingate (unpublished data); 4 = Compston (1974); Preiss et al. (1975); 5 = this study; 6 = Glikson et al. (1996); 7 = Stevens and Apak (1999); 8 = Clark et al. (2000); 9 = Sun et al. (1996); White et al. (1999)

Fitzsimons (2000) suggested that the Mesoproterozoic blocks in the Pinjarra Orogen were accreted to the western Australian margin some time after they were deformed and metamorphosed further to the south (present coordinates), but before 'stitching' of the Northampton Complex to the western Australian margin at 755 Ma by the Mundine Well dykes (Wingate and Giddings, 2000).

Late Mesoproterozoic pole positions

The virtual geomagnetic pole (GLD) for the Glenayle Dolerite agrees with the palaeopole (BBS) determined for dolerites in the western Bangemall Supergroup (Wingate, 2002). The discrepancy between the two poles (Fig. 14) is thought to be due mainly to inadequate averaging of palaeosecular variation (PSV) by the GLD pole, and reflects the small number of separate intrusions available for sampling in the flat-lying Glenayle Dolerite. The BBS result, in contrast, is based on antipodal upward- and downward-pointing palaeomagnetic directions, indicating that the magnetizations, collectively, span at least one reversal of the Earth's magnetic field and therefore are likely to have adequately averaged PSV (Wingate, 2002). This suggestion is supported by the lower concentration parameter of $k = 32$ for the western Bangemall Supergroup VGPs compared to $k = 62$ for those from the Glenayle Dolerite (Table 5).

Accepting that the Glenayle Dolerite, Prenti Dolerite, and western Bangemall Supergroup sills are coeval, palaeomagnetic data from the three areas can be combined. Giving unit weight to each of the mean Glenayle Dolerite VGPs (entry 2, Table 5) and the Prenti Dolerite VGPs (site L, Table 4), and combining them with 11 VGPs from the western Bangemall sills (table 2 of Wingate, 2002) yields a palaeopole at 97°12'E, 34°17'N (A_{95} = 7.3°, n = 13), which is within 2° of the BBS palaeopole based on the western Bangemall Supergroup data alone. Results from the Glenayle Dolerite corroborate the BBS palaeopole and improve its reliability by demonstrating that much of the Capricorn Orogen has remained essentially undeformed and (magnetically) unaltered since at least 1070 Ma.

Late Proterozoic palaeolatitudes

The inclination of the tilt-corrected palaeomagnetic direction for the Glenayle Dolerite is 49.8° (Table 5), which corresponds to a palaeolatitude of 30.5°N for the southeastern Collier Basin at 1070 Ma. Figure 16 shows latitudinal positions for Australia between 1140 and 755 Ma. Data from the Lakeview Dolerite of the Mount Isa Block indicate that Australia occupied high latitudes at 1140 Ma, assuming that the North, South, and West Australian cratonic assemblages were amalgamated by this time. The BBS pole from the western Bangemall Supergroup sills indicates that at c. 1070 Ma the continent had moved to low to middle latitudes, and was rotated slightly clockwise from its present orientation. The Glenayle Dolerite VGP corresponds to a position for Australia about 5° higher in palaeolatitude (dashed outline on Fig. 17) than indicated by the BBS pole. Australia occupied low latitudes and rotated slowly anticlockwise during the remainder of the Neoproterozoic and into the Palaeozoic (Wingate and Giddings, 2000; Pisarevsky et al., 2001).

Late Mesoproterozoic continental reconstructions

Reconstructions of Australia–Antarctica against either western Canada (the SWEAT hypothesis; Moores, 1991; Dalziel, 1991; Hoffman, 1991) or the western United States (the AUSWUS hypothesis; Brookfield, 1993; Karlstrom et al., 1999; Burrett and Berry, 2000) are based mainly on geological correlations, and have yet to receive quantitative support from precisely dated palaeopoles. A reconstruction similar to SWEAT or AUSWUS between Australia (including the Mawson block of Antarctica; Fitzsimons, 2000) and Laurentia (Fig. 17) cannot be achieved by matching the BBS pole (or the Glenayle Dolerite VGP) with the 1100 to 1020 Ma Laurentian apparent polar wander path, indicating that neither fit is viable at 1070 Ma. Superimposing the 1070 Ma BBS palaeopole for Australia (Table 5, entry 4) and an interpolated 1070 Ma pole position for Laurentia (Fig. 17) permits a reconstruction — AUSMEX (Australia–Mexico)

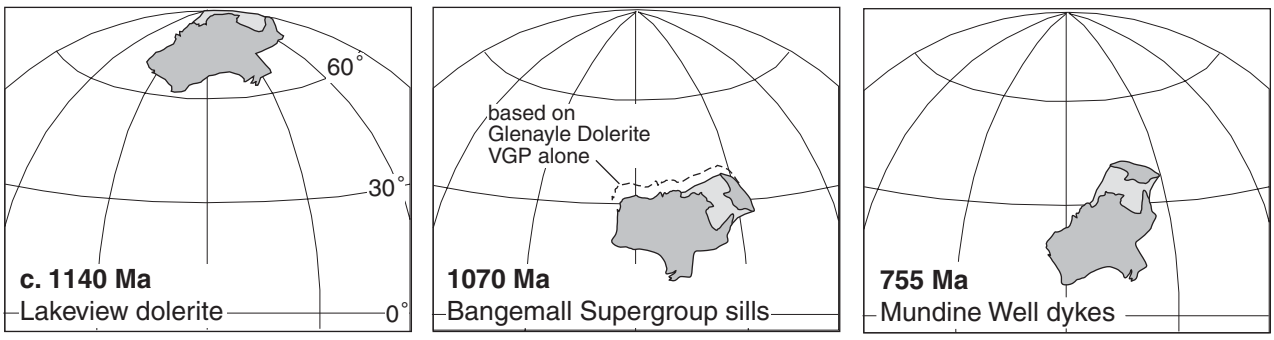

Figure 16. Late Proterozoic palaeolatitudes for Australia, based on palaeopoles for the Lakeview Dolerite of the Mount Isa Block (Tanaka and Idnurm, 1994; Claoue-Long, J., 2002, written comm.), dolerite sills of the western Bangemall Supergroup (Wingate, 2002), and the Mundine Well dyke swarm (Wingate and Giddings, 2000). Also shown (dashed outline) is the palaeoposition of Australia based on the Glenayle Dolerite virtual geomagnetic pole (VGP)

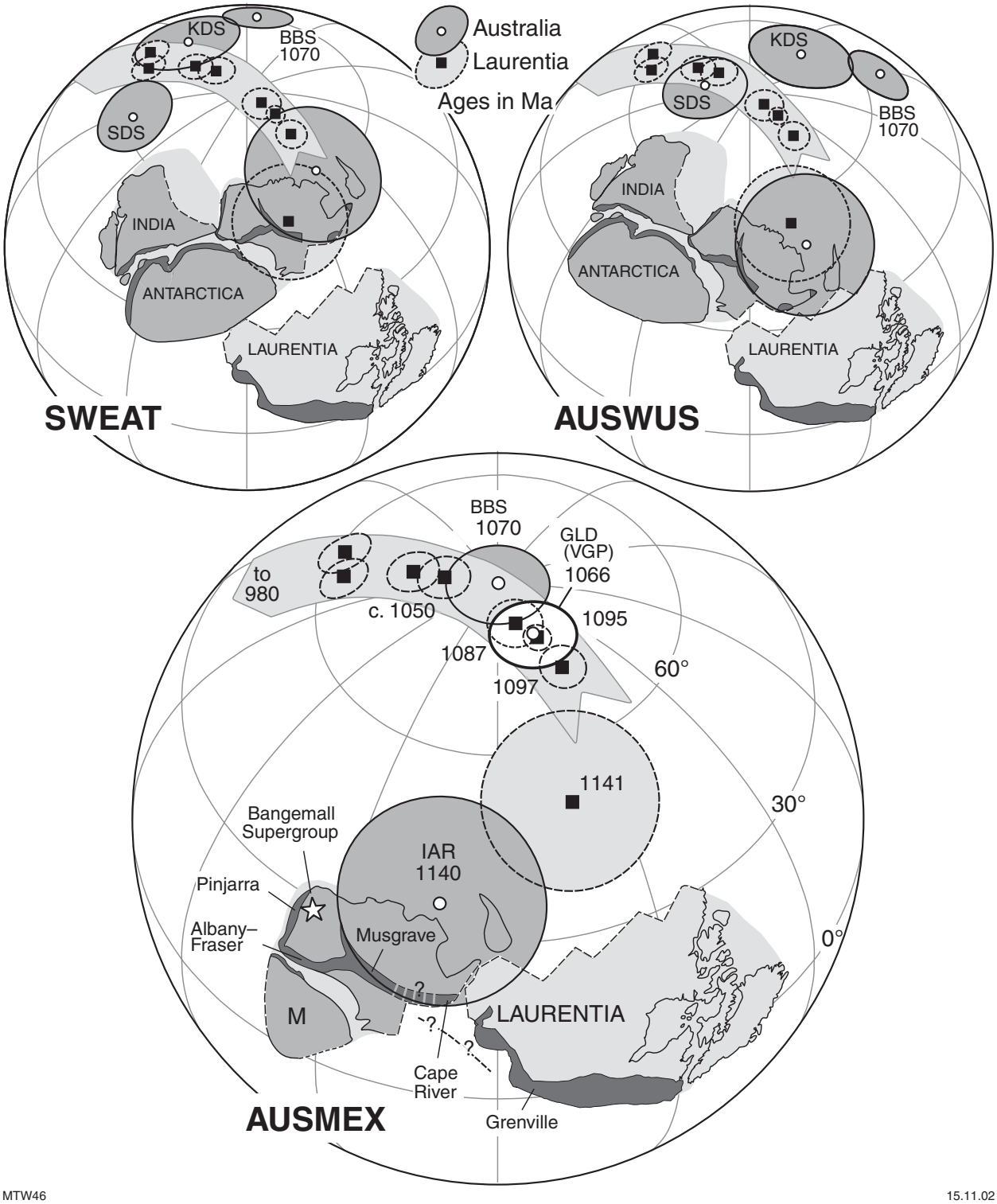

Figure 17. Late Mesoproterozoic to mid-Neoproterozoic reconstructions of East Gondwanaland (Australia + East Antarctica + India) and Laurentia, according to the SWEAT and AUSWUS hypotheses. Previous late Mesoproterozoic palaeopoles for Australia, from the Stuart dykes (SDS, Idnurm and Giddings, 1988) and Kulgera sills (KDS, Camacho et al., 1991), are less reliable than the 1070 ± 6 Ma BBS pole from dolerite sills in the western Bangemall Supergroup (Wingate et al., 2002). A reconstruction similar to SWEAT or AUSWUS cannot be achieved by matching the BBS pole with any part of the 1100 to 1050 Ma Laurentian apparent polar wander (APW) path. Based on the BBS pole, a possible reconstruction, AUSMEX, between Australia and Laurentia at 1070 Ma places the Grenville and Cape River provinces at similar palaeolatitudes. The virtual palaeomagnetic pole GLD, from the Glenayle Dolerite, is in agreement with the BBS pole, and supports the AUSMEX reconstruction. Rotation parameters and details of Australian and Laurentian palaeopoles are described in Wingate et al. (2002). Late Mesoproterozoic 'Grenville-age' mobile belts are labelled. M is the Mawson block of East Antarctica (Fitzsimons, 2000). Poles are shown with A_{95} confidence circles; arbitrary lines of longitude are 30° apart

— that closely aligns late Mesoproterozoic orogenic belts in northeastern Australia and southernmost Laurentia (Wingate et al., 2002).

However, palaeomagnetic data for the 1235 Ma Sudbury dykes (Palmer et al., 1977) place Laurentia at low latitudes, whereas new palaeomagnetic results (Wingate, M.T.D., unpublished data) for the 1212 ± 10 Ma Fraser dyke swarm (Wingate et al., 2000) and c. 1.2 Ga metamorphic rocks of the Albany–Fraser Orogen (Pisarevsky and Harris, 2001) place Australia at high latitudes. Although the 25 million-year difference in age between the two palaeopoles could mask significant latitudinal motion of either continent, the large difference in palaeolatitudes makes any direct connection between the two continents at that time less likely, and implies that they may have moved independently during late Mesoproterozoic (Grenville-age) orogenic events. Imprecise data suggest that both continents occupied high latitudes at 1140 Ma. By 1070 Ma Australia and Laurentia had moved to low-latitude positions, possibly in an arrangement similar to AUSMEX. These observations imply that Palaeoproterozoic and Mesoproterozoic geological similarities between Australia and Laurentia may be fortuitous, and that the Pacific Ocean did not form by separation of eastern Australia and western Laurentia.

Dolerite sills in the Yerrida Basin

During the same field expedition in which the Glenayle Dolerite was sampled for palaeomagnetism and U–Pb geochronology, samples were collected for a reconnaissance palaeomagnetic survey of dolerite sills in the Palaeoproterozoic Yerrida Basin. The results of rock magnetic and palaeomagnetic analyses of these samples are presented here.

Geological background

The Palaeoproterozoic Yerrida Basin developed along the northern margin of the Yilgarn Craton, and forms part of the southern margin of the Capricorn Orogen (Fig. 1). The present geometry of the Yerrida Basin is the result of deformation, probably during the 1.83 – 1.78 Ga Capricorn Orogeny (Tyler and Thorne, 1990; Occhipinti et al., 1999), which involved southeast-directed thrusting of the Bryah Group over the Yerrida Group along the northeast-trending Goodin Fault (Fig. 18), deforming the northwestern margin of the Yerrida Basin (Pirajno and Adamides, 2000; Pirajno and Occhipinti, 2000).

The Yerrida Basin (Fig. 18) contains a lower sedimentary succession (Windplain Group), overlain by a volcano-sedimentary succession (Mooloogool Group). The Windplain Group (Juderina and Johnson Cairn Formations) unconformably overlies Archaean basement rocks and contains sandstone, shale, carbonate, and evaporitic rocks, thought to have been deposited in shallow epicontinental seas, with local development of sabkha environments (Pirajno et al., 1995, 1996; Pirajno et al., in press). Continued extension led to development of a rift basin (Mooloogool rift), within which a succession of siliciclastic sedimentary and mafic igneous rocks, the Mooloogool Group (Doolgunna, Thaduna, Killara, and Maraloou Formations; Pirajno et al., 1998; Pirajno and Adamides, 2000), was accumulated. The Doolgunna and Thaduna Formations represent rift-fill facies, and include conglomerates, megabreccias, and turbidites. These formations interdigitate with each other and with mafic igneous rocks of the Killara Formation, indicating that high-energy sedimentation was contemporaneous with volcanism (Pirajno and Adamides, 2000; Pirajno and Occhipinti, 2000; Pirajno et al., in press). Volcanic activity was followed by deposition of sulfidic shale, laminated siltstone, and minor sandstone and carbonate of the Maraloou Formation under stagnant and anoxic conditions, probably in a lacustrine setting (Pirajno and Adamides, 2000). In the western part of the basin, mafic lavas and sills of the Killara Formation were emplaced into unconsolidated wet sediments of the Maraloou Formation, whereas in the east the Maraloou Formation unconformably overlies the Killara Formation, suggesting contemporaneous block faulting (Pirajno et al., 1998).

The Killara Formation contains about 1000 m of commonly unmetamorphosed, flat-lying or gently dipping, subaerial and subaqueous flows, sills, and dykes (Dawes and Pirajno, 1998; Pirajno et al., 1998). Dolerite sills and dykes of the Killara Formation intruded all formations of the Yerrida Basin (Pirajno and Adamides, 2000; Pirajno and Occhipinti, 2000). The igneous rocks have calc-alkaline to tholeiitic basaltic and basaltic andesite compositions, and have negative Nb anomalies and high Ce/Yb values (Pirajno et al., 1998). Multiple basalt flows have been recognized, with unweathered flow tops and without intercalated sedimentary material, indicating rapid eruption (Pirajno and Occhipinti, 2000). These geochemical and geological observations suggest that the volcanic rocks of the Killara Formation are continental flood basalts (Dawes and Pirajno, 1998; Pirajno et al., 1998).

Sedimentary rocks of the Yerrida Group were deposited between about 2.2 and 1.84 Ga. A Pb–Pb age of 2173 ± 63 Ma reported for stromatolitic carbonate at the base of the Windplain Subgroup was interpreted as the age of deposition (Woodhead and Hergt, 1997). Rasmussen and Fletcher (2002) reported an age of 1843 ± 10 Ma for emplacement of a subvolcanic dolerite sill within the Maraloou Formation, based on SHRIMP U–Pb dating of monazite that developed in contact metamorphosed shale. Evidence that the sill intruded wet sediment indicates that the U–Pb age approximates the time of deposition of the Maraloou Formation (Rasmussen and Fletcher, 2002).

Sampling and analytical procedures

Procedures for sampling and palaeomagnetic analysis are similar to those described above for the Glenayle Dolerite. Between eight and fourteen core samples were collected at each of four sites in dolerite of the Killara Formation

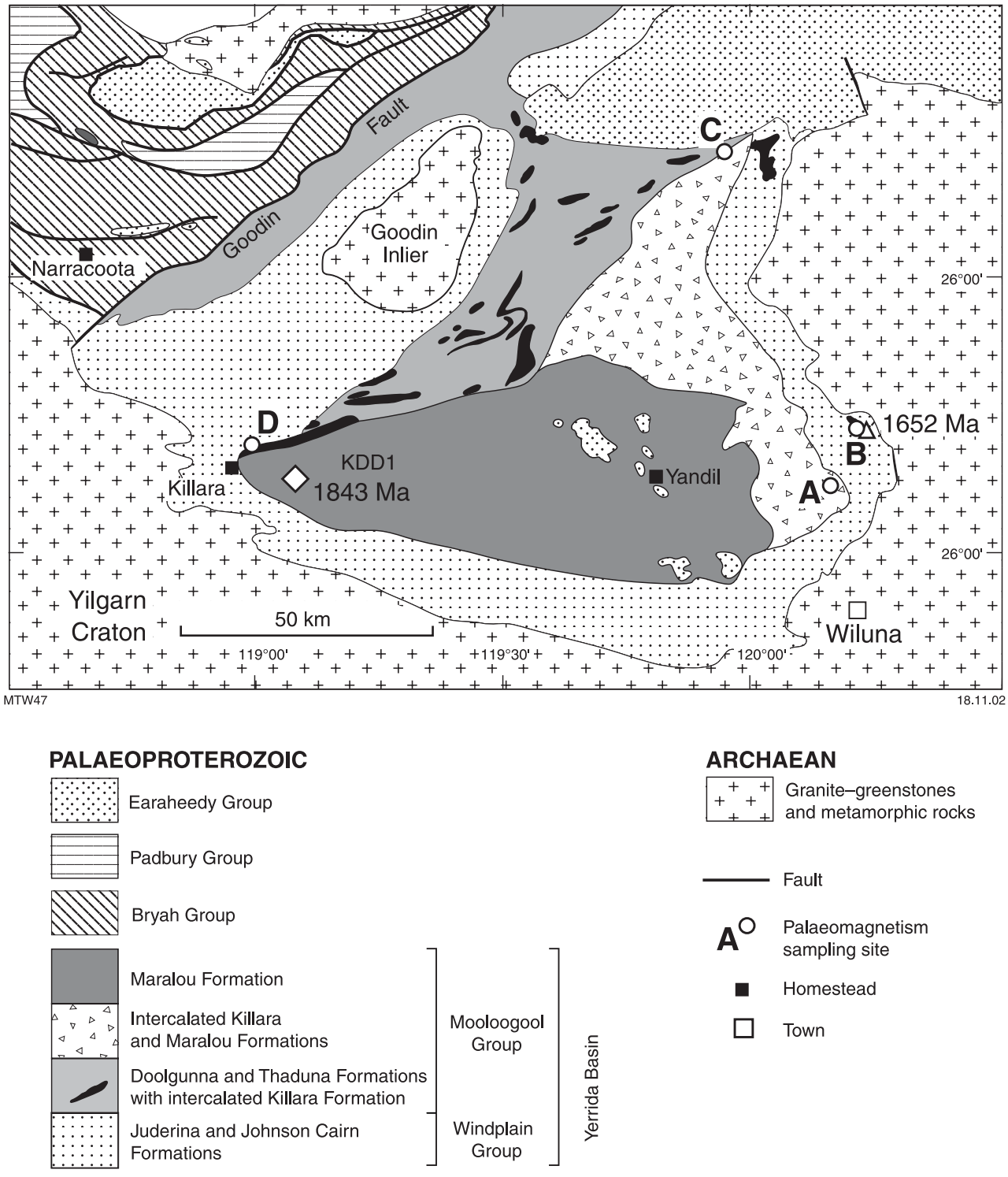

Figure 18. Simplified geological map of the Yerrida Basin and parts of the Bryah and Padbury Basins (after Pirajno and Adamides, 2000; Pirajno and Occhipinti, 2000), showing locations of sites sampled for palaeomagnetism. Dolerite sills are dated at 1843 ± 10 Ma (diamond symbol: U–Pb monazite, crystallization age; Rasmussen and Fletcher, 2002) and 1652 ± 23 Ma (triangle: K–Ar potassium feldspar, minimum crystallization age; Nelson, 2002)

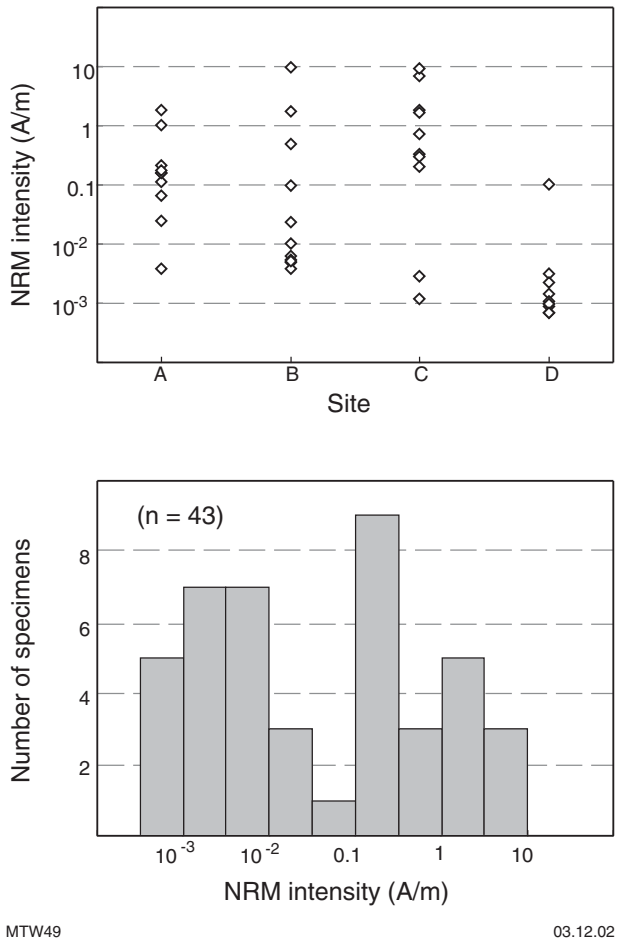

Figure 19. Natural remanent magnetization (NRM) intensities measured in samples from four sites in dolerite sills of the Killara Formation

(Fig. 18, Appendix 2). One specimen from each core sample was subjected to detailed AF demagnetization; duplicate specimens from two samples from each site were demagnetized thermally.

Petrography

The Killara Formation consists of intrusive and extrusive mafic rocks. The bulk of the intrusive rocks are ophitic to subophitic augite dolerite, with or without orthopyroxene. Some sills are composed of hypersthene dolerite. Plagioclase is labradorite in composition ($An_{55–70}$). Secondary quartz may be present and, in places, is associated with chlorite and epidote. The main opaque minerals are leucoxene and ilmenite, the latter commonly in skeletal form. Dolerites show variable degrees of alteration and epidotization. Plagioclase is commonly saussuritized, and pyroxene is serpentinized.

Extrusive rocks consist of aphyric tholeiitic basalt, less commonly microporphyritic or glomeroporphyritic, and contain normative albite, diopside, hypersthene, and olivine. Augite forms phenocrysts and is in the groundmass. Aphyric basalts have a variolitic or intersertal to hyalopilitic texture with plagioclase microlites, augite grains, and minor secondary quartz. Some porphyritic varieties contain millimetre-scale augite, and plagioclase phenocrysts are set in a very fine grained feathery groundmass of clinopyroxene, plagioclase, and devitrified glass. Plagioclase varies from fresh grains to grains that are altered completely to clay minerals and chlorite. Accessory ilmenite shows various stages of alteration to leucoxene. Vesicles contain calcite, chlorite, epidote, quartz, and, in places, feldspar or granophyric quartz and feldspar, or zeolites (?stilbite).

Results

Measurements were conducted on 43 specimens from 35 core samples. Natural remanent magnetization (NRM) intensities are weak and distributed bimodally, with about half of the measurements grouped above 0.1 A/m and the remainder below 0.01 A/m (Fig. 19). Specimens from site D are particularly weak, with intensities averaging about 1 mA/m. By comparison, these values are three orders of magnitude lower than NRM intensities measured in samples of Glenayle Dolerite (Fig. 7).

The NRMs are directed either inconsistently or commonly northward with moderate upward inclinations, similar to Earth's present field direction in the study area. Most specimens are magnetically 'soft', and magnetizations are effectively randomized after treatment at AF fields of 20 to 30 mT or temperatures of 300 to 400°C (Figs 20 and 21). In several cases the magnetizations are stable at higher fields or temperatures, although little consistency in direction is exhibited within results for each site (Fig. 22).

An essential mineral in most dolerite intrusions is relatively pure (>95%) magnetite, which forms during cooling by oxyexsolution of high-temperature titanomagnetite. Although magnetite-bearing rocks typically have relatively high bulk susceptibilities, the susceptibilities of four Killara Formation dolerite samples are very low, and detailed susceptibility versus temperature curves (Fig. 23) are probably dominated by contributions from paramagnetic minerals (Tarling and Hrouda, 1993), and little or no trace of a signature attributable to magnetite is apparent. These curves can be contrasted with those for samples of Glenayle Dolerite (Fig. 10), in which susceptibility is dominated completely by the contribution from magnetite.

Thermal demagnetization curves, summarized in Figure 24, show distributed unblocking temperatures between 100 and 350°C for seven samples; one sample from site C yielded a demagnetization curve that indicates unblocking of magnetite above 500°C. The magnetizations of two samples are reduced considerably in intensity by treatment at 100 and 200°C, suggesting that goethite is the dominant remanence carrier in these samples. The magnetizations of the remaining samples are effectively destroyed by 350°C, suggesting that their remanence may be carried mainly by maghemite, in which case the apparent unblocking reflects inversion to hematite (Dunlop and Özdemir, 1997).

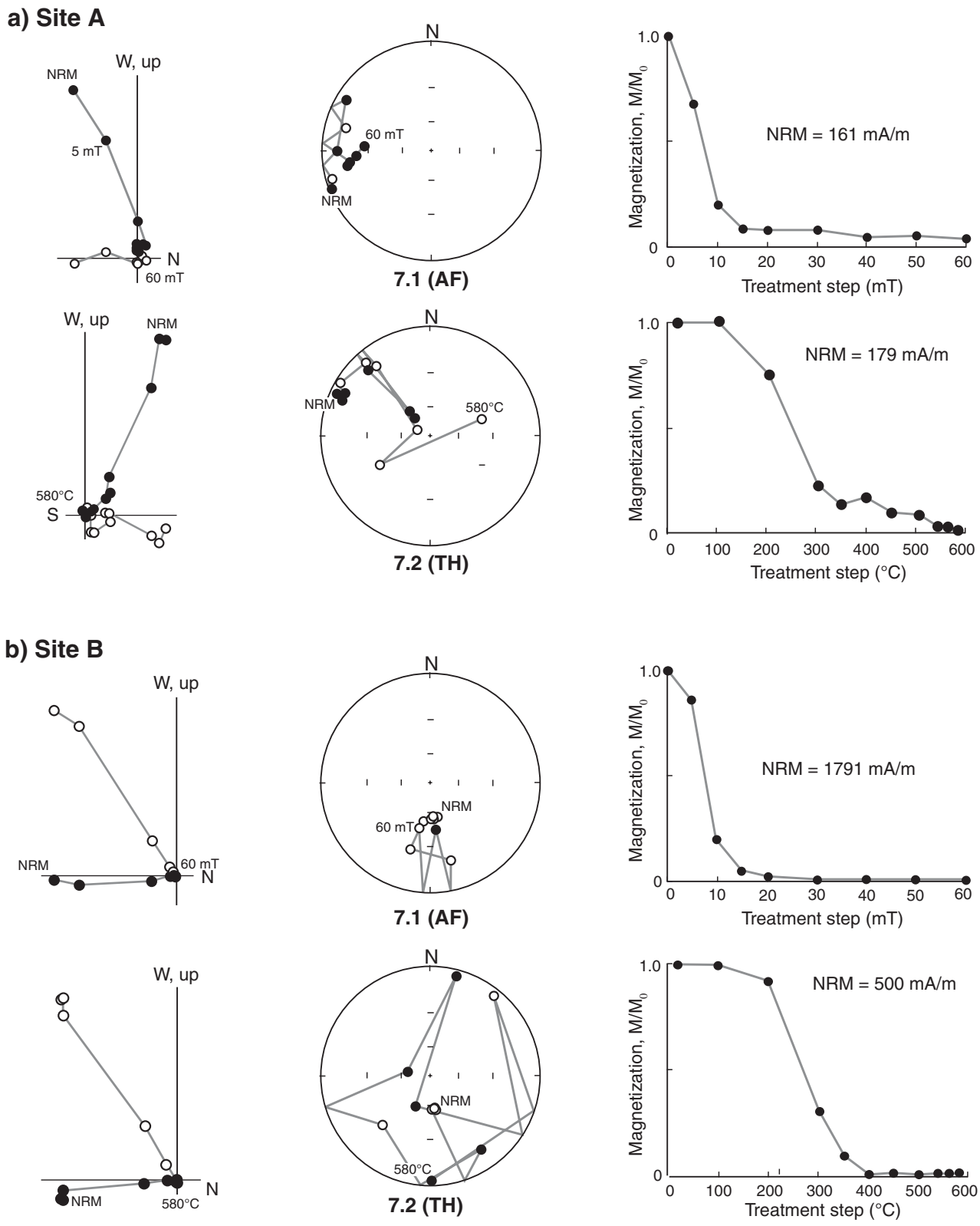

Figure 20. Examples of alternating field (AF) and thermal (TH) demagnetization of two samples of a single core from each of sites A and B in the Killara Formation. Orthogonal projections show trajectories of vector endpoints during progressive demagnetization (open/closed symbols represent vertical/horizontal planes). Open/closed symbols in lower hemisphere equal-angle stereographic projections indicate upward/downward pointing directions. Demagnetization curves show changes in magnetization intensity during treatment. Reference frame is present horizontal. The natural remanent magnetization (NRM) intensity is the initial intensity measured before demagnetization

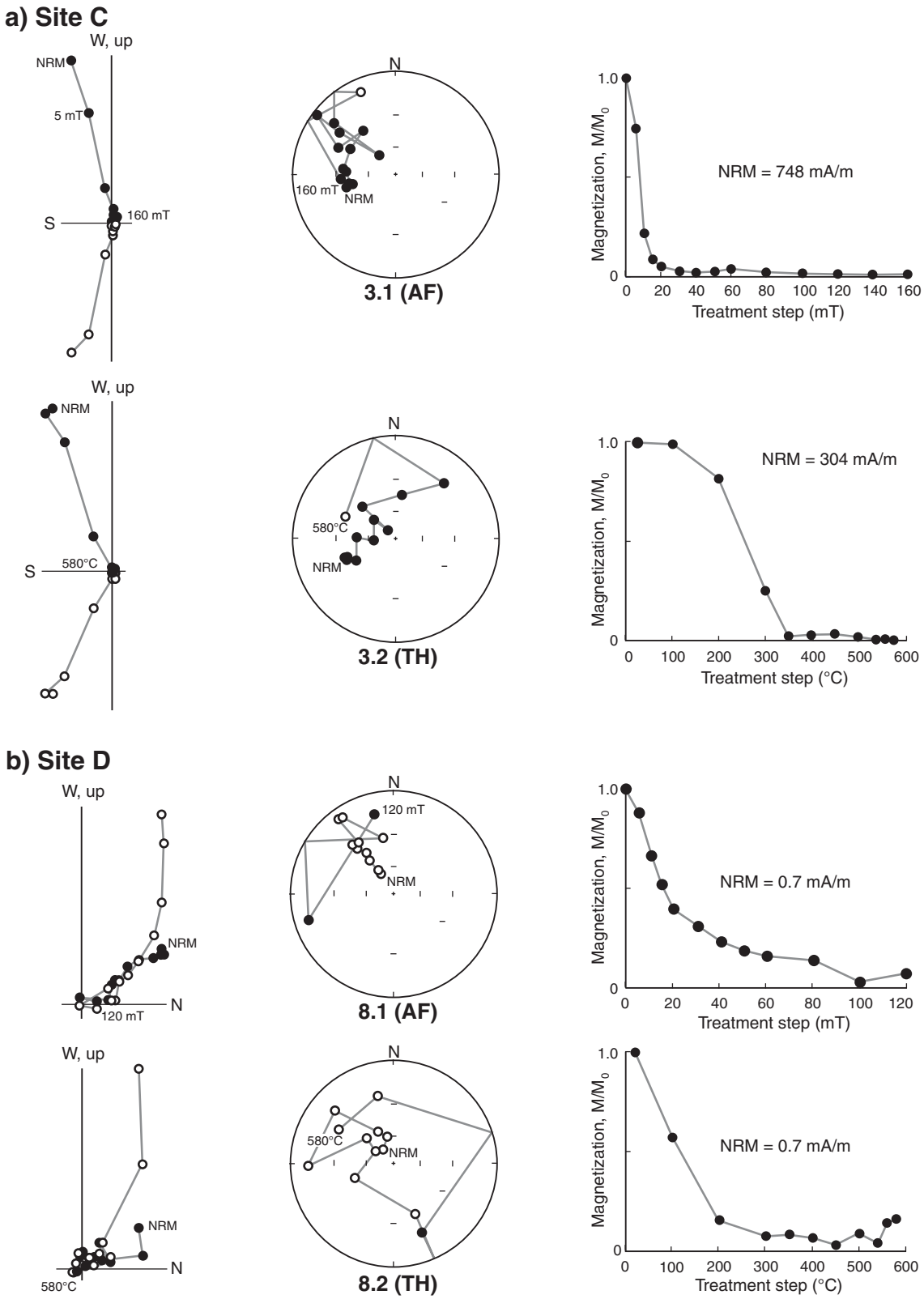

MTW50 03.12.02

Figure 21. Examples of alternating field (AF) and thermal (TH) demagnetization of two samples of a single core from each of sites C and D in the Killara Formation. Orthogonal projections show trajectories of vector endpoints during progressive demagnetization (open/closed symbols represent vertical/horizontal planes). Open/closed symbols in lower hemisphere equal-angle stereographic projections indicate upward/downward pointing directions. Demagnetization curves show changes in magnetization intensity during treatment. Reference frame is present horizontal. The natural remanent magnetization (NRM) intensity is the initial intensity measured before demagnetization

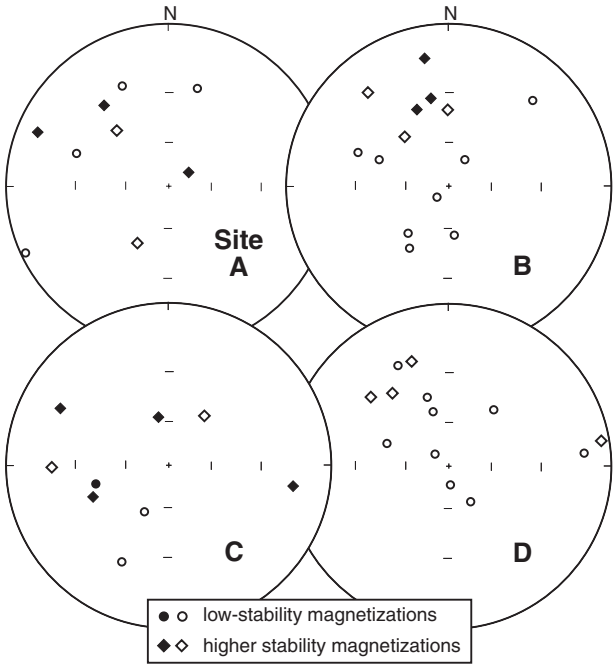

Figure 22. Palaeomagnetic directions measured at sites A to D in dolerite sills of the Killara Formation. Open/closed symbols in lower-hemisphere equal-angle stereographic projections indicate upward/downward pointing directions. Higher stability magnetizations are those isolated above treatment to 30 mT or 400°C

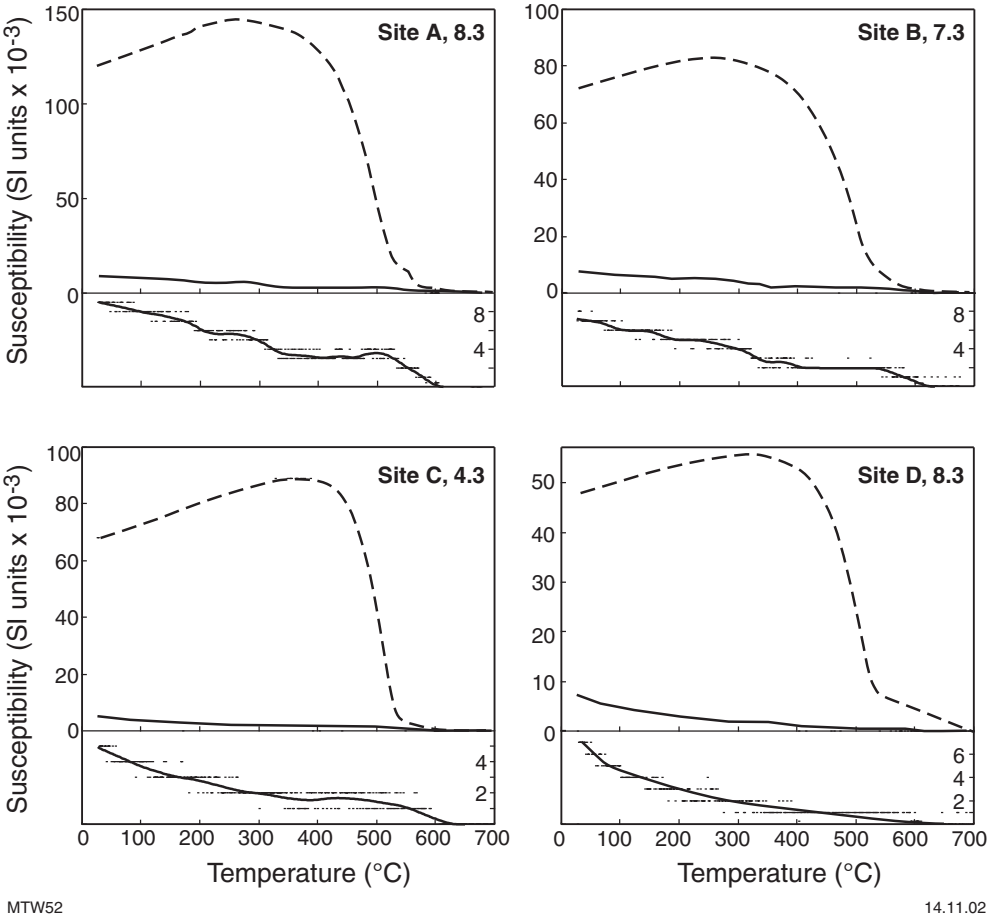

Figure 23. Variation of low-field susceptibility with temperature for four samples of dolerite from the Killara Formation (heating = solid curves; cooling = dashed curves). The lower part of each plot shows the heating curve and actual measurements with an expanded vertical scale. Cooling curves indicate production of magnetite during heating, probably the result of high-temperature breakdown of nonmagnetic silicate minerals

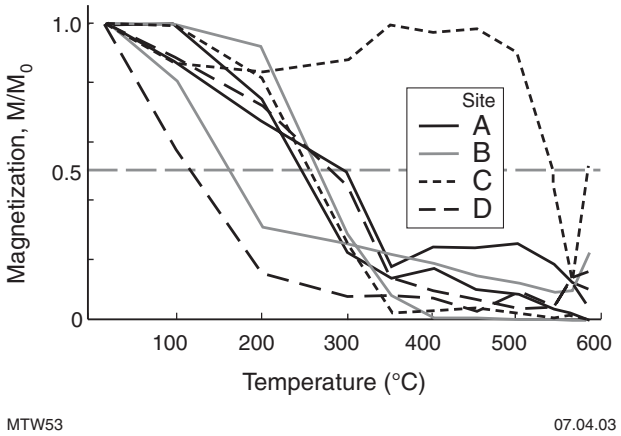

Figure 24. Thermal demagnetization curves for two samples from each site in the Killara Formation

Summary and discussion

Palaeomagnetic and rock magnetic measurements were conducted on samples from four sites in dolerite sills of the Killara Formation in the Yerrida Basin (Fig. 18). The majority of magnetizations are of low coercivity, becoming unstable after treatment to 20 or 30 mT. Unblocking temperatures for seven of eight samples subjected to thermal demagnetization are lower than 350°C. One sample analyzed thermally appears to carry a magnetite-based remanence, but whether this is a primary or secondary magnetization is unknown. Detailed susceptibility versus temperature measurements indicate that magnetite is largely absent from these samples. Magnetization directions are highly dispersed, both within and between sites, although several cluster close to the direction of Earth's present field in the study area. Together with petrographic evidence for moderate to extensive alteration, these observations indicate that the magnetizations of the Killara Formation dolerite sills are either chemical remagnetizations (CRMs), acquired during alteration or weathering, or, in some cases, recent viscous overprints (VRMs). Alteration may have resulted from fluid-related metasomatism during the 1.83 to 1.78 Ga Capricorn Orogeny. High directional dispersion suggests that the CRM overprints were acquired over an extended interval or at different times. No coherent palaeomagnetic component could be determined for the Killara Formation sills (Fig. 22). Based on the results for these pilot samples, the Palaeoproterozoic rocks of the Yerrida Basin are less than ideal targets for future palaeomagnetic studies.

Acknowledgements

This research was conducted at the Tectonics Special Research Centre, at the University of Western Australia, Perth, supported in part by a Grant-in-Aid from the Geological Survey of Western Australia. Field vehicles and logistical support were supplied by the Geological Survey of Western Australia. Nien Schwarz assisted with field sampling. Palaeomagnetic analyses were carried out at the palaeomagnetic laboratory of the School of Earth and Geographical Sciences at the University of Western Australia. The U–Pb measurements were conducted using the SHRIMP II ion microprobe in Perth, operated by a consortium consisting of the University of Western Australia, Curtin University of Technology, and the Geological Survey of Western Australia, with the support of the Australian Research Council. Greg Black and Sergei Pisarevsky assisted with palaeomagnetic measurements. Constructive comments on the manuscript were provided by Sergei Pisarevsky and David Nelson.

References

BAGAS, L., GREY, K., HOCKING, R. M., and WILLIAMS, I. R., 1999, Neoproterozoic successions of the northwest Officer Basin: a reappraisal: Western Australia Geological Survey, Annual Review 1998–99, p. 39–44.

BLACK, L. P., KINNY, P. D., and SHERATON, J. W., 1991, The difficulties of dating mafic dykes: an Antarctic example: Contributions to Mineralogy and Petrology, v. 109, p. 183–194.

BROOKFIELD, M. E., 1993, Neoproterozoic Laurentia–Australia fit: Geology, v. 21, p. 683–686.

BROSSART, P. J., MEIER, M., OBERLI, F., and STEIGER, R. H., 1986, Morphology versus U–Pb systematics in zircon: a high-resolution isotopic study of a zircon population from a Variscan dyke in the Central Alps: Earth and Planetary Science Letters, v. 78, p. 339–354.

BRUGUIER, O., BOSCH, D., PIDGEON, R. T., BYRNE, D. I., and HARRIS, L. B., 1999, U–Pb geochronology of the Northampton Complex, Western Australia — evidence for Grenvillian sedimentation, metamorphism and deformation and geodynamic implications: Contributions to Mineralogy and Petrology, v. 136, p. 258–272.

BURRETT, C., and BERRY, R., 2000, Proterozoic Australia – Western United States (AUSWUS) fit between Laurentia and Australia: Geology, v. 28, p. 103–106.

CAMACHO, A., SIMONS, B., and SCHMIDT, P. W., 1991, Geological and palaeomagnetic significance of the Kulgera Dyke Swarm, N.T., Australia: Geophysical Journal International, v. 107, p. 37–45.

CLARK, D. J., HENSEN, B. J., and KINNY, P. D., 2000, Geochronological constraints for a two-stage history of the Albany–Fraser Orogen, Western Australia: Precambrian Research, v. 102, p. 155–183.

COMMANDER, D. P., MUHLING, P. C., and BUNTING, J. A., 1982, Stanley, W.A.: Western Australia Geological Survey, 1:250 000 Geological Series Explanatory Notes, 19p.

COMPSTON, W., 1974, The Table Hill volcanics of the Officer Basin — Precambrian or Paleozoic?: Journal of the Geological Society of Australia, v. 21, p. 403–411.

CUMMING, G. L., and RICHARDS, J. R., 1975, Ore lead isotope ratios in a continuously changing Earth: Earth and Planetary Science Letters, v. 28, p. 155–171.

DALZIEL, I. W. D., 1991, Pacific margins of Laurentia and East Antarctica – Australia as a conjugate rift pair: Evidence and implications for an Eocambrian supercontinent: Geology, v. 19, p. 598–601.

DAWES, P. D., and PIRAJNO, F., 1998, Geology of the Mount Bartle 1:100 000 sheet: Western Australia Geological Survey, 1:100 000 Geological Series Explanatory Notes, 26p.

DUNLOP, D. J., and ÖZDEMIR, Ö., 1997, Rock magnetism: fundamentals and frontiers: United Kingdom, Cambridge University Press, 573p.

ERNST, R. E., and BARAGAR, W. R. A., 1992, Evidence from magnetic fabric for the flow pattern of magma in the Mackenzie giant radiating dyke swarm: Nature, v. 356, p. 511–513.

FISHER, R. A., 1953, Dispersion on a sphere: Proceedings of the Royal Society of London, v. A217, p. 295–305.

FITZSIMONS, I. C. W., 2000, Grenville-age basement provinces in East Antarctica: Evidence for three separate collisional orogens: Geology, v. 28, p. 879–882.

GLIKSON, A. Y., STEWART, A. J., BALLHAUS, C. G., CLARKE, G. L., FEEKEN, E. H. J., LEVEN, J. H., SHERATON, J. W., and SUN, S.-S., 1996, Geology of the western Musgrave Block, central Australia, with particular reference to the mafic–ultramafic Giles Complex: Australian Geological Survey Organisation, Bulletin 239, 206p.

HARRIS, L. B., 1995, Correlation between the Albany, Fraser, and Darling Mobile Belts of Western Australia and Mirnyy to Windmill Islands in the East Antarctic Shield: Implications for Proterozoic Gondwanaland reconstructions: Geological Society of India, Memoir 34, p. 47–71.

HEAMAN, L. M., and LeCHEMINANT, A. N., 1993, Paragenesis and U–Pb systematics of baddeleyite (ZrO_2): Chemical Geology, v. 110, p. 95–126.

HEAMAN, L. M., LECHEMINANT, A. N., and RAINBIRD, R. H., 1992. Nature and timing of Franklin igneous events, Canada: Implications for a Late Proterozoic mantle plume and the break-up of Laurentia: Earth and Planetary Science Letters, v. 109, p. 117–131.

HOCKING, R. M., and JONES, J. A., 2002, Geology of the Methwin 1:100 000 sheet: Western Australia Geological Survey, 1:100 000 Geological Series Explanatory Notes, 35p.

HOCKING, R. M., JONES, J. A., PIRAJNO, F., and GREY, K., 2000, Stratigraphic revision of Proterozoic rocks in the Earaheedy Basin and nearby areas: Western Australia Geological Survey, Record 2000/16, 22p.

HOFFMAN, P. F., 1991, Did the breakout of Laurentia turn Gondwanaland inside-out? Science, v. 252, p. 1409–1412.

IDNURM, M., and GIDDINGS, J. W., 1988, Australian Precambrian polar wander: a review: Precambrian Research, v. 40, p. 61–88.

KARLSTROM, K. E., HARLAN, S. S., WILLIAMS, M. L., McLELLAND, J., GEISSMAN, J. W., and ÅHÄLL, K., 1999, Refining Rodinia: geologic evidence for the Australia – Western U.S. connection in the Proterozoic: GSA Today, v. 9, p. 1–7.

KIRSCHVINK, J. L., 1980, The least-squares line and plane and the analysis of palaeomagnetic data: Geophysical Journal of the Royal Astronomical Society, v. 62, p. 699–718.

LOFGREN, G., 1980, Experimental studies on the dynamic crystallization of silicate melts, *in* Physics of magmatic processes *edited by* R. B. HARGRAVES: U.S.A., Princeton University Press, p. 487–551.

McFADDEN, P. L., 1982, Rejection of palaeomagnetic observations: Earth and Planetary Science Letters, v. 61, p. 392–395.

MARTIN, D. McB., and THORNE, A. M., 2002, Revised litho-stratigraphy of the Mesoproterozoic Bangemall Supergroup on the Edmund and Turee Creek 1:250 000 sheets, Western Australia: Western Australia Geological Survey, Record 2002/15, 27p.

MARTIN, D. McB., THORNE, A. M., and COPP, I. A., 1999, A provisional revised stratigraphy for the Bangemall Group on the Edmund 1:250 000 sheet: Western Australia Geological Survey, Annual Review 1998–99, p. 51–55.

MOORES, E. M., 1991, Southwest U.S. – East Antarctic (SWEAT) connection: a hypothesis: Geology, v. 19, p. 425–428.

MUHLING, P. C., and BRAKEL, A. T., 1985, Geology of the Bangemall Group — the evolution of an intracratonic Proterozoic basin: Western Australia Geological Survey, Bulletin 128, 266p.

MYERS, J. S., SHAW, R. D., and TYLER, I. M., 1996, Tectonic evolution of Proterozoic Australia: Tectonics, v. 15, p. 1431–1446.

NELSON, D. R., 1998, Compilation of SHRIMP U–Pb zircon geochronological data, 1997: Western Australia Geological Survey, Record 1998/2, 242p.

NELSON, D. R., 2002, Compilation of geochronology data, 2001: Western Australia Geological Survey, Record 2002/2, 282p.

OCCHIPINTI, S. A., SHEPPARD, S., TYLER, I. M., and NELSON, D., 1999, Deformation and metamorphism during the c. 2000 Ma Glenburgh Orogeny and the c. 1800 Ma Capricorn Orogeny: Geological Society of Australia, Abstracts, v. 56, p. 26–29.

PALMER, H. C., MERZ, B. A., and HAYATSU, A., 1977, The Sudbury Dykes of the Grenville Front region: paleomagnetism, petrochemistry, and K–Ar age studies: Canadian Journal of Earth Sciences, v. 14, p. 1867–1887.

PIRAJNO, F., and ADAMIDES, N. G., 2000, Geology and mineralization of the Palaeoproterozoic Yerrida Basin, Western Australia: Western Australia Geological Survey, Report 60, 43p.

PIRAJNO, F., ADAMIDES, N. G., OCCHIPINTI, S. A., SWAGER, C. P., and BAGAS, L., 1995, Geology and tectonic evolution of the early Proterozoic Glengarry Basin, Western Australia: Western Australia Geological Survey, Annual Review 1994–95, p. 71–80.

PIRAJNO, F., BAGAS, L., SWAGER, C. P., OCCHIPINTI, S. A., and ADAMIDES, N. G., 1996, A reappraisal of the stratigraphy of the Glengarry Basin: Western Australia Geological Survey, Annual Review 1995–96, p. 81–87.

PIRAJNO, F., and HOCKING, R. M., 2001, Mudan, W.A. Sheet 3247: Western Australia Geological Survey, 1:100 000 Geological Series.

PIRAJNO, F., and HOCKING, R.M., 2002, Glenayle, W.A. Sheet 3347: Western Australia Geological Survey, 1:100 000 Geological Series.

PIRAJNO, F., JONES, A., HOCKING, R. M., and HALILOVIC, J., in press, Geology and tectonic evolution of the eastern Capricorn Orogen, Western Australia: Precambrian Research.

PIRAJNO, F., MORRIS, P. A., and WINGATE, M. T. D., 2002, A possible large igneous province (LIP) in central Western Australia: implications for mineralization models: 16th Australian Geological Convention; Geological Society of Australia, Abstracts, v. 67, p. 140.

PIRAJNO, F., and OCCHIPINTI, S. A., 2000, Three Palaeoproterozoic basins — Yerrida, Bryah and Padbury — Capricorn Orogen, Western Australia: Australian Journal of Earth Sciences, v. 47, p. 675–688.

PIRAJNO, F., OCCHIPINTI, S. A., and SWAGER, C. P., 1998, Geology and tectonic evolution of the Palaeoproterozoic Bryah, Padbury, and Yerrida Basins (formerly Glengarry Basin), Western Australia: implications for the history of the south-central Capricorn Orogen: Precambrian Research, v. 90, p. 119–140.

PISAREVSKY, S. A., and HARRIS, L. B., 2001, Determination of magnetic anisotropy and a ca. 1.2 Ga palaeomagnetic pole from the Bremer Bay area, Albany Mobile Belt, Western Australia: Australian Journal of Earth Sciences, v. 48, p. 101–112.

PISAREVSKY, S. A., LI, Z.-X., GREY, K., and STEVENS, M. K., 2001, A palaeomagnetic study of Empress 1A, a stratigraphic drillhole in the Officer Basin; evidence for a low-latitude position of Australia in the Neoproterozoic: Precambrian Research, v. 110, p. 93–108.

PREISS, W. V., JACKSON, M. J., PAGE, R. W., and COMPSTON, W., 1975, Regional geology, stromatolite biostratigraphy, and isotopic data bearing on the age of a Precambrian sequence near Lake Carnegie, Western Australia: Geological Society of Australia, 1st Australian Geological Convention, p. 92–93.

PULLAIAH, G., IRVING, E., BUCHAN, K. L., and DUNLOP, D. J., 1975, Magnetization changes caused by burial and uplift: Earth and Planetary Science Letters, v. 28, p. 133–143.

RASMUSSEN, B., and FLETCHER, I. R., 2002, Indirect dating of mafic intrusions by SHRIMP U–Pb analysis of monazite in contact metamorphosed shale: an example from the Palaeoproterozoic Capricorn Orogen, Western Australia: Earth and Planetary Science Letters, v. 197, p. 287–299.

REISCHMANN, T., 1995, Precise U/Pb age determination with baddeleyite (ZrO_2), a case study from the Phalaborwa Igneous Complex, South Africa: South African Journal of Geology, v. 98, p. 1–4.

SCHMIDT, P. W., 1993, Palaeomagnetic cleaning strategies: Physics of the Earth and Planetary Interiors, v. 76, p. 169–178.

SHEPPARD, S., and SWAGER, C. P., 1999, Geology of the Marquis 1:100 000 sheet: Western Australia Geological Survey, 1:100 000 Geological Series Explanatory Notes, 21p.

STEIGER, R. H., and JÄGER, E., 1977, Subcommission on geochronology: convention on the use of decay constants in geo- and cosmochronology: Earth and Planetary Science Letters, v. 36, p. 359–362.

STEVENS, M. K., and APAK, S. N., 1999, GSWA Empress 1 and 1A well completion report, Yowalga Sub-basin, Officer Basin, Western Australia: Western Australia Geological Survey, Record 1999/4, 110p.

SUN, S.-S., SHERATON, J. W., GLIKSON, A. Y., and STEWART, A. J., 1996, A major magmatic event during 1050–1080 Ma in central Australia and an emplacement age for the Giles Complex: AGSO Research Newsletter, v. 17, p. 9–10.

TANAKA, H., and IDNURM, M., 1994, Palaeomagnetism of Proterozoic mafic intrusions and host rocks of the Mt Isa Inlier, Australia: Precambrian Research, v. 69, p. 241–258.

TARLING, D. H., and HROUDA, F., 1993, The magnetic anisotropy of rocks: Chapman and Hall, London, 217p.

TYLER, I. M., and THORNE, A. M., 1990, The northern margin of the Capricorn Orogen, Western Australia — an example of an early Proterozoic collision zone: Journal of Structural Geology, v. 12, p. 685–701.

VAN DER VOO, R., 1990, The reliability of palaeomagnetic data: Tectonophysics, v. 184, p. 1–9.

WALTON, D., 1980, Time–temperature relations in the magnetization of assemblies of single-domain grains: Nature, v. 286, p. 245–247.

WHITE, R. S., 1992, Magmatism during and after continental breakup, *in* Magmatism and the causes of continental breakup *edited by* B. C. STOREY, T. ALABASTER, and R. J. PANKHURST: United Kingdom, Geological Society, Special Publication 68, p. 1–16.

WHITE, R. W., CLARKE, G. L., and NELSON, D. R., 1999, SHRIMP U–Pb dating of Grenville-age events in the western part of the Musgrave Block, central Australia: Journal of Metamorphic Geology, v. 17, p. 465–481.

WILLIAMS, I. R., 1990, Bangemall Basin, *in* Geology and mineral resources of Western Australia: Western Australia Geological Survey, Memoir 3, p. 308–329.

WILLIAMS, I. R., 1995, Trainor, W.A. (2nd edition): Western Australia Geological Survey, 1:250 000 Geological Series Explanatory Notes, 31p.

WINGATE, M. T. D., 1997, Testing Precambrian continental reconstructions using ion microprobe U–Pb baddeleyite geochronology and palaeomagnetism of mafic igneous rocks: Canberra, Australian National University, PhD thesis (unpublished).

WINGATE, M. T. D., 2000, Ion microprobe U–Pb zircon and baddeleyite ages for the Great Dyke and its satellite dykes, Zimbabwe: South African Journal of Geology, v. 103, p. 74–80.

WINGATE, M. T. D., 2002, Age and palaeomagnetism of dolerite sills intruded into the Bangemall Supergroup on the Edmund 1:250 000 map sheet, Western Australia: Western Australia Geological Survey, Record 2002/4, 48p.

WINGATE, M. T. D., CAMPBELL, I. H., COMPSTON, W., and GIBSON, G. M., 1998, Ion microprobe U–Pb ages for Neoproterozoic basaltic magmatism in south-central Australia and implications for the breakup of Rodinia: Precambrian Research, v. 87, p. 135–159.

WINGATE, M. T. D., CAMPBELL, I. H., and HARRIS, L. B., 2000, SHRIMP baddeleyite age for the Fraser Dyke Swarm, southeast Yilgarn Craton, Western Australia: Australian Journal of Earth Sciences, v. 47, p. 309–313.

WINGATE, M. T. D., and COMPSTON, W., 2000, Crystal orientation effects during ion microprobe analysis of baddeleyite: Chemical Geology, v. 168, p. 75–97.

WINGATE, M. T. D., and GIDDINGS, J. W., 2000., Age and palaeomagnetism of the Mundine Well dyke swarm, Western Australia: implications for an Australia – Laurentia connection at 755 Ma: Precambrian Research, v. 100, p. 335–357.

WINGATE, M. T. D., PISAREVSKY, S. A., and EVANS, D. A. D., 2002, Rodinia connections between Australia and Laurentia: no SWEAT, no AUSWUS?: Terra Nova, 14, p. 121–128.

WOODHEAD, J. D., and HERGT, J. M., 1997, Application of the 'double spike' technique to Pb-isotope geochronology: Chemical Geology, v. 138, p. 311–321.

ZHAO, J.-X., and McCULLOCH, M. T., 1993, Sm–Nd mineral isochron ages of Late Proterozoic dyke swarms in Australia: evidence for two distinct events of mafic magmatism and crustal extension: Chemical Geology, v. 109, p. 341–354.

Appendix 1

Sample site descriptions — southeast Collier Basin and Earaheedy Basin

Grid references refer to the Geocentric Datum of Australia 1994 (GDA94) using Map Grid Australia (MGA) coordinates, Zone 51.

Site A (north of Yallum Bore)

Coordinates: Lat. 25°25'16"S, Long. 122°14'53"E, STANLEY* (SG 51-6; MGA 424400E 7188218N).

Location: Southeastern edge of a low dolerite hill, about 1.7 km from Yallum Bore on a bearing of 024°; about 3.9 km northwest of Yallum Hill.

Geological relations: Dolerite sill intruding the Coonabildie Formation.

Palaeomagnetic samples: 8 core samples of massive, medium-grained dolerite, collected over 145 m along edge of outcrop area.

Site B (Weld Spring)

Coordinates: Lat. 25°1'12"S, Long. 121°35'10"E, STANLEY (SG 51-6; MGA 357307E 7232089N).

Location: Low dolerite outcrops exposed within creek bed, about 200 m south of track, about 400 m south of Weld Spring (Canning Stock Route well number 9).

Geological relations: Flat-lying dolerite sill intruding the Coonabildie Formation.

Palaeomagnetic samples: 9 core samples of medium-grained dolerite collected over 150 m within creek bed.

Site C (northwest of Midway Bore)

Coordinates: Lat. 25°4'55"S, Long. 121°42'54"E, STANLEY (SG 51-6; MGA 370399E 7225362N).

Location: Low rubbly outcrop on south-facing slope of low dolerite hill, 250 m north of track, 4.4 km northwest of Midway Bore.

Geological relations: Dolerite sill intruding the Coonabildie Formation.

Palaeomagnetic samples: 9 core samples of medium-grained dolerite collected over 130 m along an east–west trend (approximately parallel to track).

Site D (Digby Hill)

Coordinates: Lat. 25°11'35"S, Long. 121°53'17"E, STANLEY (SG 51-6; MGA 387961E 7213255N).

* Capitalized names refer to standard 1:250 000 map sheets.

Location: Low rubbly outcrop on south-facing slope of low dolerite hill, 150 m north of track, 1.4 km east-southeast of Humpty Doo Bore; 1.1 km west of geochronology sample site 152661 (see below).

Geological relations: Dolerite sill intruding the Coonabildie Formation.

Palaeomagnetic samples: 12 core samples of medium-grained dolerite collected over 100 m along an east–west trend (approximately parallel to track).

Site E (west of Dailys Bore)

Coordinates: Lat. 25°5'28"S, Long. 121°0'54"E, STANLEY (SG 51-6; MGA 400692E 7224638N).

Location: Outcrop along small stream bed draining the west side of dolerite hill, 150 m north of track, 2.2 km west of Dailys Bore.

Geological relations: Dolerite sill intruding the Coonabildie Formation.

Palaeomagnetic samples: 8 core samples of fine- to medium-grained dolerite collected over 40 m along east–west trending stream.

Site F (south of Gap Well)

Coordinates: Lat. 25°11'38"S, Long. 122°13'19"E, STANLEY (SG 51-6; MGA 421647E 7213393N).

Location: Low rubbly outcrop on east side of low dolerite hill, 200 m west of track, 900 m south of Gap Well.

Geological relations: Dolerite sill intruding the Coonabildie Formation.

Palaeomagnetic samples: 9 core samples of fine- to medium-grained dolerite collected over m along an north–south trend.

Site G (south of Gap Well)

Coordinates: Lat. 25°11'38"S, Long. 122°13'37"E, STANLEY (SG 51-6; MGA 422148E 7213366N).

Location: Low rubbly outcrop on west side of low dolerite hill, 100 m east of track, 1.2 km south of Gap Well.

Geological relations: Dolerite sill intruding the Coonabildie Formation.

Palaeomagnetic samples: 5 core samples of very fine grained dolerite collected over 100 m along a north–south trend.

Site H (south of One Gum Bore)

Coordinates: Lat. 25°13'52"S, Long. 122°32'17"E, STANLEY (SG 51-6; MGA 453487E 7209408N).

Location: Rubbly outcrop on southwest side of prominent dolerite hill, 200 m east of track, 1.2 km south of One Gum Bore.

Geological relations: Dolerite sill intruding the Coonabildie Formation.

Palaeomagnetic samples: 7 core samples of fine-grained dolerite collected over 160 m along a northwest trend.

Site I (west of One Gum Bore)

Samples collected in two areas:

Area A

Coordinates: Lat. 25°12'47"S, Long. 122°29'2"E, STANLEY (SG 51-6; MGA 447977E 7211389N).

Location: Low rubbly outcrop 50 m south of track, 6.5 km west of One Gum Bore.

Geological relations: Dolerite sill intruding the Coonabildie Formation.

Palaeomagnetic samples: 6 core samples of very fine grained dolerite collected over a 15 by 40 m area.

Area B

Coordinates: Lat. 25°12'40"S, Long. 122°28'26" E, STANLEY (SG 51-6; MGA 446989E 7211597N).

Location: Outcrops in and adjacent to bed of creek draining northeast slopes of prominent dolerite hill, about 200 m south of track, 1.1 km west of Area A.

Geological relations: Dolerite sill intruding the Coonabildie Formation.

Palaeomagnetic samples: 6 core samples of very fine grained dolerite collected over 120 m along creek.

Site J (southeast of Glenayle Homestead)

Coordinates: Lat. 25°16'34"S, Long. 122°5'53"E, STANLEY (SG 51-6; MGA 409211E 7204221N).

Location: Outcrops in and along bed of well-incised creek draining southwestern slopes of a prominent hill, 1.4 km northeast of the Glenayle–Carnegie Road, 5.7 km southeast of Glenayle Homestead.

Geological relations: Upper contact of dolerite sill intruding the Coonabildie Formation.

Palaeomagnetic samples: 8 core samples of very fine grained to aphanitic dolerite collected over 130 m in creek bed.

Site K (Canning Stock Route)

Coordinates: Lat. 24°55'41"S, Long. 121°36'22"E, TRAINOR (SG 51-2; MGA 359205E 7242347N).

Location: 10 km south of No. 10 Well on the Canning Stock Route.

Geological relations: Dolerite sill intruding the Coonabildie Formation.

Palaeomagnetic samples: 8 block samples of medium-grained dolerite, collected over 20 m along edge of outcrop area.

Site L (south of Prenti Downs Homestead)

Coordinates: Lat. 26°31'37"S, Long. 122°49'26"E, KINGSTON (SG 51-10; MGA 482455E 7065989N).

Location: Moderately weathered outcrops in steep gully along creek, adjacent to southwestern side of Virgins Road, at first curve of road south of Prenti Downs Homestead.

Geological relations: Lower contact of basalt sill intruding sandstone of the Princess Ranges Formation.

Palaeomagnetic samples: 7 core samples of aphanitic basalt collected over 60 m along northeastern bank of creek.

Geochronology sample 152661

Coordinates: Lat. 25°11'42"S, Long. 121°53'56"E, STANLEY (SG 51-6; MGA 389079E 7213000N).

Location: 2.5 km east-southeast of Humpty Doo Bore, on the station track between Glenayle Homestead and Weld Spring; 1.1 km east of palaeomagnetism site D (see above).

Geological relations: Dolerite sill intruding the Coonabildie Formation.

Geochronology sample: About 20 kg of unweathered, medium-grained granophyric dolerite collected from outcrops immediately north of the station track.

Geochronology sample 171741

Coordinates: Lat. 25°11'42"S, Long. 121°53'56"E, STANLEY (SG 51-6; MGA 389079E 7213000N).

Location: 2.5 km east-southeast of Humpty Doo Bore, on the station track between Glenayle Homestead and Weld Spring; 1.1 km east of palaeomagnetism site D (see above).

Geological relations: Dolerite sill intruding the Coonabildie Formation.

Geochronology sample: About 20 kg of unweathered, medium-grained granophyric dolerite collected from the same outcrop area as palaeomagnetic samples at site K.

Appendix 2

Sample site descriptions — Yerrida Basin

Grid references refer to the Geocentric Datum of Australia 1994 (GDA94) using Map Grid Australia (MGA) coordinates, Zones 50 and 51.

Site A (north of North Pool)

Coordinates: Lat. 26°22'41"S, Long. 120°9'50"E, WILUNA (SG 51-9; MGA 217038E 7079315N).

Location: Southwestern margin of an extensive, low dolerite hill, 8 km north of North Pool; 300 m east of track; bearing 280° to Telstra telecommunications tower.

Geological relations: Dolerite sill (Killara Formation) intruding Juderina Formation.

Palaeomagnetic samples: 8 core samples of massive, medium-grained dolerite, collected over 135 m along edge of outcrop area.

Site B (Canning Stock Route)

Samples collected in two areas 650 m apart.

Area 1

Coordinates: Lat. 26°16'41"S, Long. 120°13'12"E, WILUNA (SG 51-9; MGA 222327E 7090571N).

Location: Northeast-facing slope of prominent dolerite hill, 150 m west of Canning Stock Route (CSR), 3.8 km along CSR from start at Wiluna North Road.

Geological relations: Dolerite sill (Killara Formation) intruding Juderina Formation.

Palaeomagnetic samples: 6 core samples of medium-grained dolerite collected over 70 m on east slope of hill.

Area 2

Coordinates: Lat. 26°16'52"S, Long. 120°13'26"E, WILUNA (SG 51-9; MGA 222795E 7090232N).

Location: South-facing slope of prominent dolerite hill, about 500 m east of CSR, 3.8 km along CSR from start at Wiluna North Road.

Geological relations: Dolerite sill (Killara Formation) intruding Juderina Formation.

Palaeomagnetic samples: 5 core samples of medium-grained dolerite collected over 40 m around outcrop blasted previously with explosives.

Site C (Wiluna North Road)

Coordinates: Lat. 25°46'12"S, Long. 119°56'53"E, PEAK HILL (SG 50-8; MGA 795696E 7146509N).

Location: Low rubbly outcrop area on either side of Wiluna North Road (WNR), 106.5 km from Wiluna along WNR.

Geological relations: Dolerite sill (Killara Formation) intruding Maraloou Formation.

Palaeomagnetic samples: 5 core samples of medium-grained dolerite collected over 50 m on southwestern side of WNR; 5 core samples of medium-grained dolerite collected over 120 m on northeastern side of WNR.

Site D (northeast of Killara Station)

Coordinates: Lat. 26°18'25"S, Long. 118°59'42"E, GLENGARRY (SG 50-12; MGA 699201E 7088805N).

Location: Rubbly outcrop along north-trending creek, about 500 m east of north–south station track, 6 km east-northeast of Killara Homestead.

Geological relations: Mafic sill or flow of Killara Formation.

Palaeomagnetic samples: 14 core samples of fine-grained basalt collected over 200 m along both sides of creek and in adjacent low ground and north- and northeast-facing slopes.